Michigan Institute for Plasma Science and Engineering (MIPSE)

University of Michigan & Michigan State University

4th ANNUAL
GRADUATE STUDENT SYMPOSIUM

September 25, 2013

2:30 – 7:00 pm

1200 EECS

North Campus, University of Michigan

1301 Beal Avenue

Ann Arbor, MI 48109-2122

University of Michigan
Ann Arbor, MI

Michigan Institute for Plasma Science and Engineering (MIPSE)

University of Michigan & Michigan State University

4th ANNUAL GRADUATE STUDENT SYMPOSIUM

Schedule

2:30 – 2:45	**Poster set-up**
2:45 – 3:00	Prof. Mark J. Kushner, Director of MIPSE ***Opening Remarks***
3:00 – 3:45	**Poster Session I**
4:00 – 5:00	**Special MIPSE Seminar:** **Prof. Edward Thomas,** Auburn University ***Magnetized Dusty Plasma Experiment: A User Facility for Complex Plasma Research***
5:00 – 5:45	**Poster Session II**
5:45 – 6:30	**Poster Session III**
6: 45 – 7:00	***Best Presentation Award*** **Ceremony**

Refreshments will be provided.

mipse
Michigan Institute for
Plasma Science and Engineering

Wednesday
September 25, 2013
4:00 pm
Room 1200
EECS Building

Prof. Edward Thomas

Auburn University

Magnetized Dusty Plasma Experiment: A User Facility for Complex Plasma Research

A dusty (or complex) plasma is a four-component system consisting of electrons, ions, neutral atoms, and charged, nanometer to micrometer sized particles (“dust”). Because the dust grains are charged, they participate in plasma dynamics and can be used to study transport, instabilities, and charging properties of plasmas. One important area that has not been extensively studied is magnetized dusty plasmas. Even though dust grains in lab experiments have several thousand charges, the charge-to-mass ratio is low. It is technically challenging to achieve full magnetization of ions, electrons, and the charged dust grains. In 2011, the NSF funded the first mid-scale, multi-user research facility for the study of dusty plasmas. The mission of the Magnetized Dusty Plasma Experiment (MDPX), based at Auburn University in collaboration with the U. of Iowa and U. of California – San Diego, is to study the properties of dusty plasmas in which the magnetic force on the charged microparticles is comparable to the other plasma forces. MDPX will produce highly uniform as well as shaped magnetic fields above 4T. This presentation will provide a brief overview of the development of magnetized dusty plasma experiments, highlighting recent studies at Kiel and Garching, will discuss the capabilities and diagnostic development of MDPX, and hopefully present some of the initial measurements performed using the MDPX facility.

About the Speaker: Edward Thomas, Jr. earned the BS in Physics from the Florida Inst. of Tech., MS in Physics from MIT, and his Ph.D. in Physics from Auburn Univ. He was an Asst. Prof. at Fisk Univ. before returning to Auburn in 1999 as a faculty member in the Physics Dept. where he is now the Lawrence C. Wit Professor in the College of Sciences and Mathematics. Prof. Thomas’ group conducts experimental plasma physics research focusing on complex (dusty) plasmas, magnetized plasmas and fusion science. Prof. Thomas is active in science policy and outreach through his work with the American Physical Society, Natl. Society of Black Physicists, University Fusion Association, International Union of Radio Science, and Quality Education for Minorities; and serving on advisory committees for NSF, DOE, and research centers in the US and Europe.

Student Participants

Last Name	First Name	Institution	Poster Session	Poster number
Bardel	Charles	Michigan State University	I	1-08
Belancourt	Patrick	University of Michigan	I	1-02
Bell	Iverson	University of Michigan	III	3-05
Cai	Xiuzhang	University of Michigan	II	2-10
Choi	Maria	University of Michigan	I	1-04
Cummings	Paul	University of Michigan	II	2-02
Davis	Joshua	University of Michigan	II	2-01
Demlow	Shannon	Michigan State University	I	1-12
Dharuman	Gautam	Michigan State University	III	3-03
Dragnea	Horatiu	University of Michigan	II	2-05
Durot	Christopher	University of Michigan	III	3-09
Englesbe	Alexander	University of Michigan	I	1-07
Fein	Jeff	University of Michigan	III	3-01
Gucker	Sarah M. Nowak	University of Michigan	III	3-11
He	Zhaohan	University of Michigan	III	3-02
Jain	Mayur	Michigan State University	II	2-06
Joglekar	Archis	University of Michigan	I	1-05
Katus	Roxanne	University of Michigan	II	2-08
Liu	Peiyao	Michigan State University	III	3-06
Logue	Michael	University of Michigan	I	1-06
Muehle	Matthias	Michigan State University	II	2-09
Nad	Shreya	Michigan State University	III	3-10
Parsey	Guy	Michigan State University	I	1-01
Raymond	Anthony	University of Michigan	I	1-03
Rice	Scott	Michigan State University	II	2-03
Rittersdorf	Ian	University of Michigan	III	3-04
Sawlani	Kapil	University of Michigan	III	3-14
Sekerak	Michael	University of Michigan	I	1-11
Song	Sang-Heon	University of Michigan	I	1-10
Tang	Qi	Michigan State University	II	2-13
Tian	Peng	University of Michigan	III	3-08
Tian	Wei	University of Michigan	I	1-14
Wan	Wesley	University of Michigan	III	3-07
Wang	Jun-Chieh (Jerry)	University of Michigan	II	2-04
Weis	Matthew	University of Michigan	I	1-09
Wolf	Eric	Michigan State University	III	3-13
Yager-Elorriaga	David	University of Michigan	II	2-11

Last Name	First Name	Institution	Poster Session	Poster number
Young	Rachel	University of Michigan	III	3-12
Yucel	Abdulkadir	University of Michigan	I	1-15
Zhang	Peng	University of Michigan	II	2-12
Zhang	Yiting	University of Michigan	II	2-07
Zhao	Zhen (Tony)	University of Michigan	I	1-13

Poster Session I

1-01 **Guy Parsey**, Michigan State University
Non-Equilibrium Reaction Kinetics of an Atmospheric Pressure Microwave-Driven Plasma Torch: a Kinetic Global Model

1-02 **Patrick Belancourt**, University of Michigan
Transport of Hot Electrons along a Wire

1-03 **Anthony Raymond,** University of Michigan
Investigating the Influence of Overdense Plasma Surfaces in High Harmonic Generation from High-intensity Laser Irradiation

1-04 **Maria Choi,** University of Michigan
Modeling a Hollow Cathode Plume Plasma

1-05 **Archis Joglekar**, University of Michigan
Vlasov-Fokker-Planck Modeling of Plasma near Hohlraum Walls Heated with Nanosecond Laser Pulses Calculated Using the Ray Tracing Equations

1-06 **Michael Logue,** University of Michigan
Control of Electron Energy Distributions in Inductively Coupled Plasmas Using Tandem Sources

1-07 **Alexander Englesbe**, University of Michigan
Electrostatic Probe Measurement of Sheath Potentials with Secondary Electron Emission in a Low-density Xenon Plasma

1-08 **Charles Bardel**, Michigan State University
Increasing Efficiency of Monte Carlo Particle-Fluid Collision Calculations on GPU

1-09 **Matthew Weis**, University of Michigan
Magneto-Rayleigh-Taylor Growth and Feedthrough in Cylindrical Liners

1-10 **Sang-Heon Song**, University of Michigan
SiO_2 Etch Properties and Ion Energy Distribution in Pulsed Capacitively Coupled Plasmas Sustained in $Ar/CF_4/O_2$

1-11 **Michael Sekerak**, University of Michigan
Hall Effect Thruster Oscillatory Modes

1-12 **Shannon Demlow**, Michigan State University
Temperature Dependence of Boron Doping Efficiency

1-13 **Wei Tian**, University of Michigan
Interaction of Atmospheric Pressure Dbds with Liquid Covered Tissues

1-14 **Abdulkadir Yucel**, University of Michigan
An FMM-FFT Accelerated Hybrid Volume Surface Integral Equation Solver for Electromagnetic Analysis of Plasma-Engulfed Vehicles

1-15 **Zhen (Tony) Zhao**, University of Michigan
Phase Contrast Imaging and Characterization of X-rays Produced via Ultraintense Laser Plasma Interactions Using Coated Metallic Targets

Poster Session II

2-01 **Joshua Davis,** University of Michigan
Film Characterization of Agfa D7 and D8 x-ray Film Using a Multiple Anode X-ray Source

2-02 **Paul Cummings,** University of Michigan
Simulations for the Elucidation of Electron Beam Properties in Laser-Wakefield Acceleration Experiments via Betatron and Synchrotron-Like Radiation

2-03 **Scott Rice,** Michigan State University
Multipactor Suppression Via Secondary Modes in a Coaxial Cavity

2-04 **Jun-Chieh (Jerry) Wang ,** University of Michigan
A Microdischarge Based Pressure Sensor

2-05 **Horatiu Dragnea,** University of Michigan
Description of the Sputtered Boron Atoms in the Plume of a SPT-70 Hall Thruster

2-06 **Mayur Jain,** Michigan State University
Modeling and Simulation of Strongly Coupled Plasmas

2-07 **Yiting Zhang,** University of Michigan
Control of Ion Energy & Angular Distribution in Dual-Frequency Capacitively Coupled Plasmas

2-08 **Roxanne Katus,** University of Michigan
Statistical Analysis of the Geomagnetic Response to Different Solar Wind Drivers and the Dependence on Storm Intensity

2-09 **Matthias Muehle,** Michigan State University
Investigating the Dependencies and Limitations of High Pressure Microwave Plasma Assisted Chemical Vapor Deposition of Single Crystalline Diamond

2-10 **Xiuzhang Cai,** University of Michigan
Adaptively Matched Dual Band GPS Antenna for Variable Plasma Environments

2-11 **David Yager-Elorriaga,** University of Michigan
Development of a Compact Pulse Generator for X-Ray Backlighting of Planar Foil Ablation Experiments

2-12 **Peng Zhang,** University of Michigan
Electrical Contacts: A voltage Scale for Thermal Runaway and Issues in Measurements of Constriction Resistance

2-13 **Qi Tang ,** Michigan State University
Finite Difference Weighted Essentially Non-Oscillatory Schemes with Constrained Transport for Ideal Magnetohydrodynamics

Poster Session III

3-01 **Jeff Fein,** University of Michigan
Preliminary Investigation of the High-energy X-ray Spectrum of Pinhole Point Projection Backlighters

3-02 **Zhaohan He,** University of Michigan
Direct Control of Electron Beam from a Laser Plasma Accelerator Using Adaptive Optics with a Genetic Algorithm

3-03 **Gautam Dharuman,** Michigan State University
Quasi-Classical Study of Atomic States

3-04 **Ian Rittersdorf,** University of Michigan
Effects of Random Circuit Fabrication Errors on Small Signal Gain and Output Phase in a Traveling Wave Tube

3-05 **Iverson Bell,** University of Michigan
Studying Miniature Electrodynamic Tethers and Interaction with the Low Earth Orbit Plasma

3-06 **Peiyao Liu,** Michigan State University
Atmospheric Pressure Microwave-Powered Microplasma Source Based on Strip-Line-Like Structure

3-07 **Wesley Wan,** University of Michigan
Supersonic, Single-mode, Shockwave-driven Kelvin-Helmholtz Instability Experiment on OMEGA-EP

3-08 **Peng Tian,** University of Michigan
Microwave Excited Microplasmas at Low Pressure as a Vuv Photon Source

3-09 **Christopher Durot,** University of Michigan
Development of a Novel Time-Resolved Laser-Induced Fluorescence Technique

3-10 **Shreya Nad,** Michigan State University
Growth and Analysis of Large Undoped Single Crystal Diamond Substrates Using Microwave Plasma-Assisted Chemical Vapor Deposition

3-11 **Sarah Nowak Gucker,** University of Michigan
The Scaling of Breakdown Voltage of Air Bubbles in Liquid Water

3-12 **Rachel Young,** University of Michigan
Creating Magnetized Plasma Jets on the OMEGA Laser

3-13 **Eric Wolf,** Michigan State University
A New Field Solver For Particle-in-Cell (PIC) Methods

3-14 **Kapil Sawlani,** University of Michigan
An Experimental Study to Show the Effects of Secondary Electron Emission on Plasma Properties in Hall Thrusters

1-01

Non-Equilibrium Reaction Kinetics of an Atmospheric Pressure Microwave-Driven Plasma Torch: a Kinetic Global Model

Guy Parsey, Yaman Güçlü, John Verboncoeur and Andrew Christlieb

Michigan State University (parseygu@msu.edu, yguclu@msu.edu, johnv@msu.edu, andrewch@math.msu.edu)

In the context of microwave-coupled plasmas, within atmospheric pressure nozzle geometries, we have developed a kinetic global model (KGM) framework designed for quick exploration of parameter space. Predominantly written in Python, the KGM framework is designed in a modular format so that it can be used as a reference library of computational methods. Our final goal is understanding key reaction pathways within non-equilibrium plasma assisted combustion (PAC) and whether it is possible to alter and control said pathways. In combination with a multi-term Boltzmann solver, kinetic plasma and gas-phase chemistry are solved with iterative feedback to match observed bulk conditions from experiments; using a parameterized non-equilibrium electron energy distribution function (EEDF) to define electron-impact processes. Publicly available data is used, either from open reference databases (e.g. LXcat [1]) or datasets kindly supplied by other research groups in near CHEMKIN format [2].

The chemistry systems are initially implemented in the form of species continuity and energy equations using the symbolic Python library SymPy. A symbolic system of equations is used so as to take advantage of analytical derivatives in the creation of integration aiding Jacobians and for the sake of human readability. The KGM framework is first applied to argon and 'air' (N_2-O_2) systems as a means of assessing the soundness of made assumptions and general validity of a global model with a non-equilibrium PAC system. The test with 'air' greatly increases the complexity by incorporating a plethora of excited states (e.g. translational and vibrational excitations) and providing new reaction pathways. Included in the new excited states will be some of the important radicals necessary for combustion augmentation (e.g. atomic O states) along with examples of waste products to be reduced (e.g. N_xO_y).

The framework is then applied to plasma driven combustion mechanisms (H_2 or CH_4 with an oxidizer source) which drastically increases the range of reaction time-scales along with combustion chain mechanisms. As the reaction mechanisms become more complex, availability of data will begin to hinder model physicality, requiring analytical and/or empirical treatment of gaps in data to maintain completeness of the reaction mechanisms. This includes sheath diffusion and gas-flow losses that must be approximated in order to be relevant to a global model. Initial simulations with argon and 'air' are simple enough to solve in a brute-force manner with regards to computational integration; the more complicated systems require a more involved implementation due to standard CPU cache limitations. In order to evaluate combustion systems, the symbolic system of equations are made into numerical functions by either compiling the whole system as callable C-code or using the newly developed Python Theano library. Implementation in Theano is in the form of graph functions, which, in principle, can be more easily optimized for multi-CPU or GPU evaluation whereas the C-code will provide the fastest version for single CPU operations.

References

[1] Biagi-v8.9 and Morgan , http://www.lxcat.laplace.univ-tlse.fr, retrieved 7.4.2012
[2] Igor Adamovich (Ohio State University), private communication

1-02

Transport of Hot Electrons along a Wire

Patrick X. Belancourt [a], Anatoly Maksimchuk [b], Mario Manuel [a], Carolyn Kuranz [a],
Paul Keiter [a] and R. Paul Drake [a]

(a) Atmospheric, Oceanic and Space Science, University Of Michigan (pxb@umich.edu)
(b) Center for Ultrafast Optical Science, University of Michigan

The transport of hot electrons is important in many areas of high-energy-density science experiments from fast ignition to background signal on film. Hot electrons are needed for the final stage in the fast ignition fusion concept to heat the central, deuterium-tritium core to ignition conditions [1], and high-energy electrons might contribute to increased background noise due the bremsstrahlung emission observed in x-ray radiographs [2]. The goal of this experiment is to investigate and manipulate the transport of electrons along a wire with energies in the range of 1-5 MeV. These experiments were preformed on the T-cubed laser at the University of Michigan. The experiment consisted of the laser focused normal to a wire with image plate stacks at one end of the wire to look at the spatial profile of the electron beam and an electron spectrometer at the other end to determine the energy spectrum. The locations of the image plate and electron spectrometer were varied to investigate how the propagation length affects electron transport. The role of wire conductivity was examined by varying the wire material using tungsten, copper and plastic. Preliminary results will be presented and discussed.

References

[1] M. Tabak, et al, Phys. Plasmas. **1**, 1626 (1994).
[2] C. Kuranz, etl al, Astrophys Space Sci. **322**, 49-55 (2009).

1-03

Investigating the Influence of Overdense Plasma Surfaces in High Harmonic Generation from High-intensity Laser Irradiation

A. Raymond [a], F. Dollar [b], C. Zulick [a], P. Cummings [a], V. Chvykov [a], L. Willingale [a], V. Yanovsky [a], A. Maksimchuk [a], A. Thomas [a], K. Krushelnick [a]

(a) Center for Ultrafast Optical Science, University of Michigan, Ann Arbor, Michigan 48109-2099, USA
(b) JILA, University of Colorado, Boulder, CO 80309, USA

In recent experimental campaigns and computational surveys, high harmonic generation (HHG) has found applications as a diagnostic tool, revealing information regarding pre-plasma scale-length and in extension laser contrast [1], in addition to many applications such as a direct means by which to produce trains of attosecond pulses [2]: via filtering lower-ordered multiples of the fundamental frequency. Additional flexibility and utility may be derived by pre-shaping the target-area of the material undergoing irradiation on the micron scale, as the results of 2D PIC simulations carried out at the University of Michigan's High Field Science group imply. Specifically, micron-scale parabolic and spherically concave target geometries are investigated in regard to their ability to collimate and further refocus the reflected harmonic beam, respectively. Additionally, results are summarized from experimental investigations carried out at the same research facility with ultrafast, ultra-relativistic, and high-contrast pulses regarding the effect of the target's pre-plasma scale-length on the efficacy of the resultant reflected beam's harmonic content.

References

[1] F. Dollar, et al., Phys. Rev. Lett. 110, 175002 (2013)
[2] George D Tsakiris, et al., New Journal of Physics 8 (2006) 19

1-04

Modeling a Hollow Cathode Plume Plasma

Maria Choi and Iain D. Boyd

University of Michigan (mclan@umich.edu, iainboyd@umich.edu)

In order to acquire better understanding of detailed electron transport and cathode coupling physics that strongly affect the performance and lifetime of a Hall thruster, it is critical to develop a reliable numerical model that can capture the collision and plasma physics accurately, validated with experimental data. The partially-ionized plasma in a hollow cathode plume can be modeled using a hybrid approach consisting of the direct simulation Monte Carlo (DSMC) and the particle-in-cell (PIC) methods. The plume of the UK-10 ion thruster cathode [1] is simulated using the DSMC-PIC code called MPIC, developed in the Non-equilibrium Gas and Plasma Dynamics Lab (NGPDL) at the University of Michigan, and is compared with experimental and numerical simulation results from Ref. [1]. The effect of charge-exchange (CEX) reactions between ions and neutrals on the ion energy distribution function (IEDF) is studied. The CEX effect is also observed in the neutral number density. The evolution of IEDFs in the plume is consistent with the potential drop from the keeper exit to downstream. Lastly, the Knudsen number at the orifice inlet indicates that the future simulation domain should include more of the upstream region of the cathode in order to account for the transition regime from continuum flow to rarefied flow. This work is the first step of a progressive plan to model more complex systems such as anomalous electron transport from the cathode to anode across magnetic fields.

References

[1] Boyd, Iain D., and Mark W. Crofton. "Modeling the plasma plume of a hollow cathode." *Journal of applied physics* 95.7 (2004): 3285-3296.

1-05

Vlasov-Fokker-Planck Modeling of Plasma near Hohlraum Walls Heated with Nanosecond Laser Pulses Calculated Using the Ray Tracing Equations

A.S. Joglekar and A.G.R. Thomas

University of Michigan (archisj@umich.edu)

Here, we present 2D numerical modeling of near critical density plasma using a fully implicit Vlasov-Fokker-Planck code, IMPACTA, which includes self-consistent magnetic fields as well as anisotropic electron pressure terms in the expansion of the distribution function, as well as an implementation of the Boris CYLRAD algorithm through a ray tracing add-on package. This allows to model inverse brehmsstrahlung heating as a laser travels through a plasma by solving the ray tracing equations using the Bohm-Gross dispersion relation. Perturbations in the plasma density and temperature profile arise as a result of the high pressures and flows in the plasma. These perturbations in the plasma properties affect tbe path of the laser traveling through the plasma, and modify the heating profile accordingly. The interplay between these effects is discussed in this study and some snapshots of the intensity and temperature profiles are shown below.

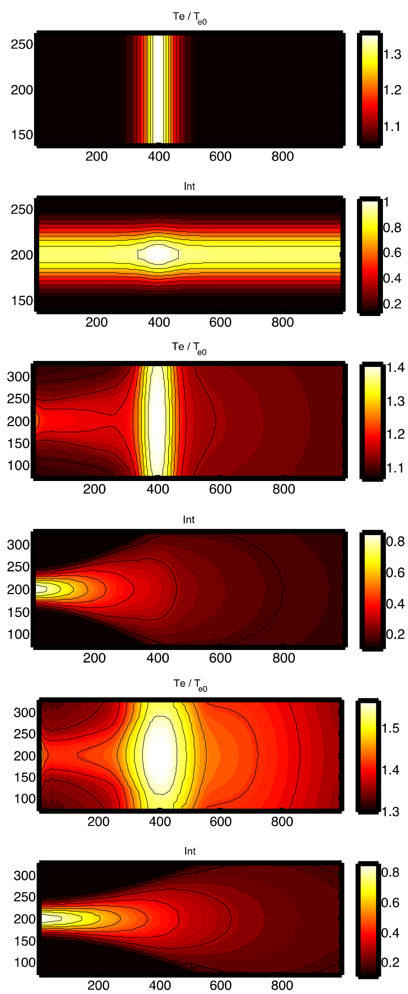

t = 0 τ_{ei}

t=1000 τ_{ei}

t = 5000 τ_{ei}

1-06

Control of Electron Energy Distributions in Inductively Coupled Plasmas Using Tandem Sources

Michael Logue [a], Mark Kushner [a], Weiye Zhu [b], Hyungjoo Shin [c], Lei Liu [b], Shyam Sridhar [b], Vincent M. Donnelly [b], Demetre Economou [b]

(a) University of Michigan (mjkush@umich.edu)
(b) University of Houston (demetre.economou@mail.uh.edu)
(c) Lam Research (shinhyungjoo@gmail.com)

In plasma materials processing, finer control of the electron energy distribution, *f(ε)*, enables better selectivity of generating reactants produced by electron impact excitation and dissociation. This is particularly important in low pressure, inductively coupled plasmas (ICPs) where dissociation products often react with surfaces before interacting with other gas phase species. Under these conditions, fluxes to surfaces are more directly a function of electron impact rate coefficients than gas phase chemistry. Externally sustained discharges are able to control *f(ε)* by, for example, augmenting ionization independent of the *f(ε)* of the bulk plasma so that *f(ε)* can be better matched to lower threshold processes. In this case, the tail the *f(ε)* is lowered. Following the same logic, introducing additional losses by external means will produce an increase in the tail of *f(ε)*. To achieve this control, a tandem (dual) ICP source has been developed. In this device, the primary (lower) source is coupled to the secondary (upper) source through a biasable grid to control the transfer of species between the two sources with the intent of controlling *f(ε)* in the primary source. A boundary electrode (BE) at the top of the system, along with the grid, can be dc biased to shift the plasma potential. This controls the energy of charged species passing into the primary source as well as ion energy distributions (IEDs) to surfaces.

Results will be discussed from a computational investigation of the control of EEDs in a tandem source ICP system at pressures of tens of mTorr. The model used in this study is the Hybrid Plasma Equipment Model (HPEM) with which *f(ε)* and IEADs as a function of position and time are obtained using a Monte Carlo simulation. *f(ε)* will be discussed while varying the relative power in the primary and secondary sources, and dc biases (BE and grids) in continuous and pulsed formats. Results from the model will be compared to experimental data of *f(ε)* obtained using a Langmuir probe.

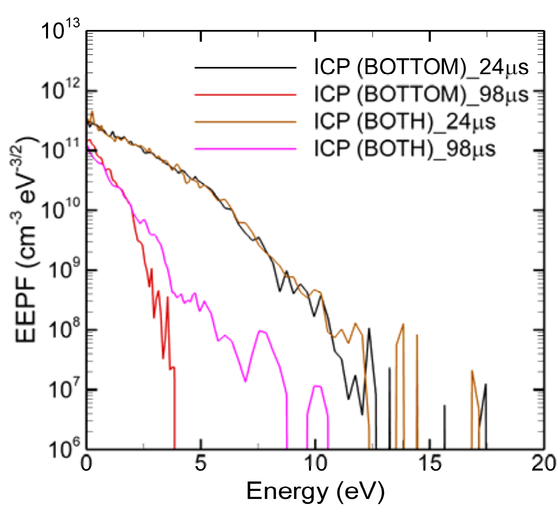

Figure 1 – Electron energy probability function (EEPF) at (r,z) = 0.5 cm, 210 cm in tandem ICP with secondary source in CW mode with 500 W, and primary ICP pulsed with a pulse-period-average (PPA) power of 100 W. EEPF's are shown at the beginning and end of plasma afterglow in primary ICP.

* Work supported by the DOE Office of Fusion Energy Science, Semiconductor Research Corp. and the National Science Foundation.

Electrostatic Probe Measurement of Sheath Potentials with Secondary Electron Emission in a Low-Density Xenon Plasma

Alexander C. Englesbe, Kapil U. Sawlani and John E. Foster

University of Michigan-Ann Arbor (aengles@umich.edu)

Knowledge of the sheath potential structure gives insight into energy transport between a plasma and its boundary. Secondary electron emission at bounding surfaces in a plasma typically reduces the magnitude of the sheath potential.[1] In an electric propulsion device such as a Hall thruster, a flux of low-temperature secondary electrons entering the main plasma will alter its electron energy distribution function.[2] The latter has a significant effect on thruster efficiency.

In these experiments, a xenon plasma is created in a cylindrical filament-driven multipole ring-cusp source that has a diameter of 17 cm. Langmuir probe measurements characterizing the source, and spatially-resolved emissive probe measurements of the sheath potential near a solid target are presented to complement planned laser-induced fluorescence (LIF) measurements of the sheath. LIF does not perturb the plasma unlike an electrostatic probe, and can make measurements much closer to the target surface.

When the beam is directed into a sheath, the spatially dependent sheath potential is recovered. The intensity of fluorescent emissions is proportional to the ion density – in this case Xe II. If the plasma density is low, the signal-to-noise ratio diminishes and it becomes difficult to generate a useable LIF signal. However, operation at low densities (10^7-10^9 cm^{-3}) is necessary in order to create a thick sheath the target, and use LIF or electrostatic probes to measure the spatial structure of the sheath potential with high resolution. The radiant emissions from the filament are the major contributor to noise in the LIF signal. Steps taken to limit the intensity of filament emissions which enter the detector are also presented.

References

[1] G.D. Hobbs and J.A. Wesson, Plasma Phys. **9**, 85 (1967).

[2] Y. Raitses, I.D. Kaganovich, A. Khrabrov, D. Sydorenko, N.J. Fisch, and A. Smolyakov. IEEE Trans. Plasma Sci. **39**, 995 (2011).

Increasing Efficiency of Monte Carlo Particle-Fluid Collision Calculations on GPU

Charles Bardel and John Verboncoeur

Electrical and Computer Engineering, Michigan State University (bardelch@msu.edu, johnv@msu.edu)

Monte Carlo collision calculations for Particle-in-Cell codes can be a very computationally and memory intensive procedure. Fortunately, this process can be set-up as an embarrassingly parallel problem for collisions with a background fluid, where the calculation of one particle does not rely on the results of another. This type of problem is well suited for GPUs, which could accelerate the computations an order of magnitude. One approach is to apply a function to every particle which involves computing the particle energy, a square root to obtain the speed, and either interpolation of tabled cross sections or computation of a curve fit for each process for every particle [1].

However, due to the nature of the hardware implementation of GPU, this simple straightforward implementation will not have the best performance fundamentally due to there being two different sets of particles: colliding and non-colliding. In this problem each of the launched groups of GPU threads, called warps, could contain members of each set of particles. Since the group is running together, the longest calculation in the group determines the running time of the entire group.

In order to achieve the best performance on the GPU the work of the particle groups to be computed must be load balanced. Where all the separate sub-tasks have approximately the same running time or operation count. This means that all the particles that will collide during time step must be known a priori. This can be achieved using the *null collisional method* [1] in which particles are selected at random using the total collision probability that is independent of particle energy and position.

On the GPU, memory requests, especially to `Global memory,' are a very expensive operation. Based on memory access optimizations from the CUDA Best Practices Guide [2] it is clear it would be best if the requested memory were collocated in memory within 128 Byte segments.

This memory optimization might severely impact the entropy of the collisions depending on the exact definition of what is meant for a particle to be collocated in memory. In this paper the memory mapping of the particles defined in [3] is used, which is designed for efficient particle-to-grid calculations. The two different optimizations are examined for a fluid background model to determine the statistical differences that arise from selecting different sizes of collocated particles. For this comparison 3 simulations are run for a domain with 10 cells. The simulations have 3 different numbers of particles corresponding to the number of the largest collocated groups, selected for null collision at $t=0$, at 1, 10, and 100. The variance of the mean thermal energies for the cells is the metric examined to determine if the energy deposited from collisions is non-uniform.

References

[1] J. P. Verboncoeur, PLASMA PHYSICS AND CONTROLLED FUSION 47, A231 (2005).
[2] Nvidia, Cuda c best practices guide, 2012.
[3] N. G. George Stantchev, William Dorland, Parallel Distrib. Comput. 68, 1339 (2008).

1-09

Magneto-Rayleigh-Taylor Growth and Feedthrough in Cylindrical Liners

Matthew Weis [a], Y. Y. Lau [a], Ronald Gilgenbach [a], Kyle Peterson [b], Mark Hess [b]

(a) University of Michigan – Ann Arbor (weisy@umich.edu)
(b) Sandia National Laboratories (mhess@sandia.gov)

Cylindrical liner implosions in the MagLIF concept [1] are susceptible to the magneto-Rayleigh-Taylor instability (MRT). In MagLIF, a pulsed power machine (such as the Z-machine at Sandia National Laboratories) is used to drive a large axial current, initiating the implosion of a metal cylindrical liner onto a pre-heated (~ 250 eV) and pre-magnetized (~ 10 T axial field) fusion fuel. During the implosion process the exterior surface of the liner is initially MRT unstable while the fuel/liner interface is stable. As the fuel becomes sufficiently compressed the liner begins to stagnate and thus, the inner surface becomes MRT unstable (as the acceleration direction has changed). Initial MRT growth on the outer surface of the liner may also feedthrough to the inner surface and provide a seed for the latter's MRT growth during the stagnation phase. Maintaining liner integrity against MRT is key to the success of MagLIF.

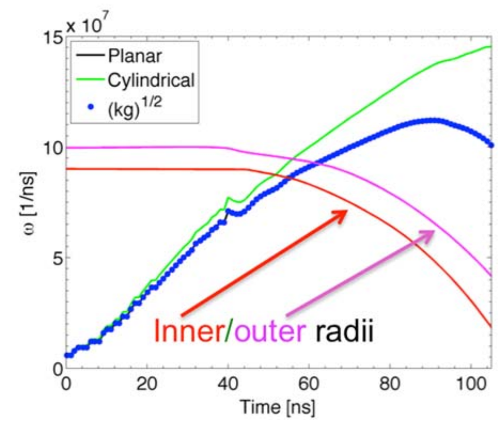

Figure 1 - MRT in cylindrical geometry (green) and planar geometry (black), and classical RT (blue) growth rates as a function of time, along with the trajectories of the inner and outer liner surface from a 1D HYDRA simulation. First, we note planar MRT growth overlaps classical RT in this instance. Second, as convergence increases, the cylindrical result shows potential for much worse growth, which is significant motivation for further study.

To characterize MRT we solve the linearized ideal MHD equations, including the presence of an axial magnetic field and the effects of sausage and kink modes. The eigenmode solution, using appropriate equilibrium profiles, allows an assessment of the local MRT growth rate and of the instantaneous feedthrough factor during the entire implosion process. In Fig. 1 we show the classical Rayleigh-Taylor growth rate and the result of our calculation along with the trajectories for a typical liner implosion [2]. We compare these analytic results along with simulation results from the LLNL code, HYDRA, to experiments on the Z-machine [2].

Of particular interest will be the high convergence/stagnation phase, which is difficult to image experimentally. Thus, we make use of our analytic theory and HYDRA simulations to characterize MRT growth. Though the purpose of the compressed axial magnetic field is to inhibit electron thermal conduction from the fuel, it is possible this field can also mitigate MRT growth at the fuel/liner interface.

This work was supported by DoE and NSF.

References

[1] S. A. Slutz, et. al, Phys. Plasmas 17, 056303 (2010).
[2] D. B. Sinars et. al. Phys. Plasmas 18, 056301 (2011).

SiO_2 etch properties and Ion Energy Distribution in Pulsed Capacitively Coupled Plasmas sustained in $Ar/CF_4/O_2$*

Sang-Heon Song [a] and Mark J. Kushner [b]

(a) Nuclear Engineering and Radiological Sciences (ssongs@umich.edu)
(b) Electrical Engineering and Computer Science (mjkush@umich.edu)
University of Michigan, Ann Arbor, MI 48109 USA

High aspect ratio (HAR) etching in microelectronics fabrication continues to be challenged to optimize plasma properties in order to maintain desired critical dimensions (CD).[1] Maintaining the CD, such as a specified angle of the side wall during etching without sacrificing etch rate requires optimizing electron densities, fluxes and energies of charged and neutral species in the plasma. A number of strategies has been attempted to achieve these goals. Employing time modulated power is one technique being attractive.[2] In one configuration of dual frequency capacitively coupled (DF-CCP), the high frequency (*HF*) power is applied to the upper electrode and low frequency (*LF*) power is applied to the lower electrode serving as the substrate which is serially connected to a blocking capacitor generating self dc bias. In this presentation, ion energy distribution and SiO_2 etch properties in a pulsed DF-CCP sustained in $Ar/CF_4/O_2$ are discussed with results from 2-dimensional plasma hydrodynamics and feature profile models. The ion energy distribution (IED) can be manipulated uniquely depending on either pulsing *LF* or *HF* power for a given size of the blocking capacitor (BC). To investigate this coupling we applied a pulsed format for *HF* and *LF* power with different duty cycles and size of BC. We found that high energy ions are dominant when pulsing the *HF* power and low energy ions are dominant when pulsing the *LF* power. Control of etch profiles will be demonstrated by combinations of pulsing *HF* and *LF* power, and BC. For example, bowing and undercut may occur when pulsing the *HF* while these effects are suppressed by pulsing the *LF*. The propensity for twisting is less when pulsing the *LF*, as shown in Fig. 1.

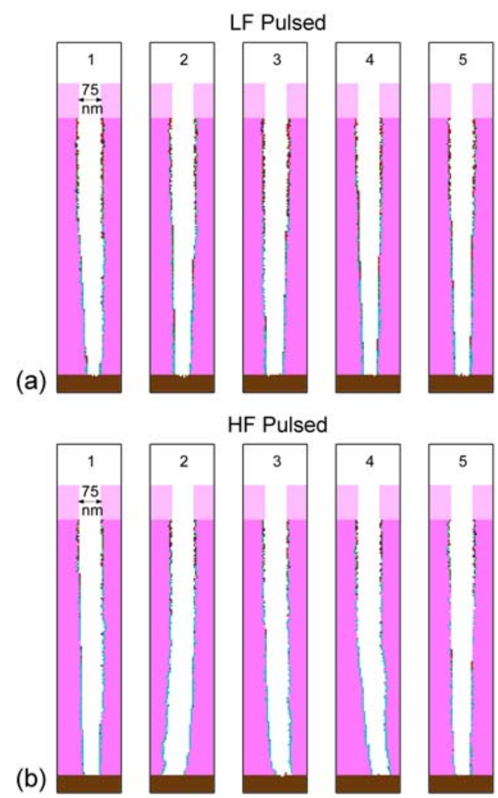

Figure 1 - SiO_2 etch profiles selected from 40 otherwise identical simulations except for using different random number seeds. (a) *LF* power is pulsed. (b) *HF* power is pulsed.

References

[1] D. Koehler and D. Fischer, ECS Trans. **13**, 47 (2008).
[2] S. Banna, A. Agarwal, G. Cunge, M. Darnon, E. Pargon, and O. Joubert, J. Vac. Sci. Technol. A **30**, 040801 (2012).

* Work supported by the Semiconductor Research Corp. and DOE Office of Fusion Energy Science.

1-11

Hall Effect Thruster Oscillatory Modes

Michael J. Sekerak, Benjamin W. Longmier and Alec D. Gallimore

University of Michigan, Department of Aerospace Engineering, Plasmadynamics and Electric Propulsion Laboratory (PEPL) (msekerak@umich.edu, longmier@umich.edu, alec.gallimore@umich.edu)

Mode transitions have been commonly observed in Hall Effect Thruster (HET) operation where a small change in a thruster operating parameter such as discharge voltage, magnetic field or mass flow rate causes the thruster discharge current mean value and oscillation amplitude to increase significantly.[1] These transitions greatly affect thruster performance and electron transport across magnetic field lines.[2] A recent investigation induced mode transitions in a 6-kW-class HET called the H6 by varying the magnetic field intensity while holding all other operating parameters constant.[3] Measurements are acquired with ion saturation probes and ultra-fast imaging in order to quantify the changes in plasma oscillations within the discharge channel and near field plasma plume. Two distinct operational modes are identified: global and local oscillation modes.

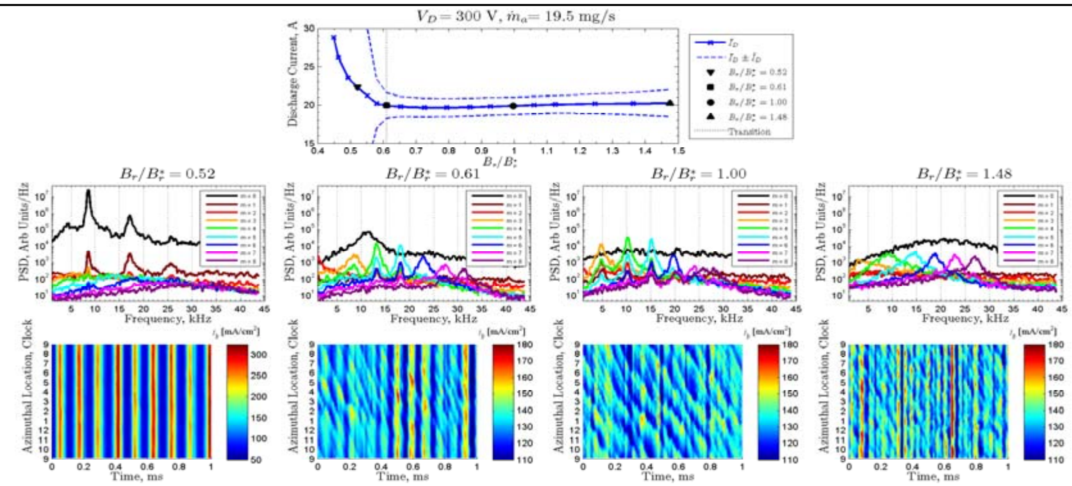

Figure 1 B-field sweep for 300 V discharge voltage, 19.5 mg/s anode flow rate showing mode transition at $B_r/B_r^* = 0.61$. Discharge current mean and oscillation amplitude are shown with the transition at the top. Middle row plots are HIA Power Spectral Densities showing different spoke orders and bottom row plots are discharge current density for 1 ms.

In global mode (B_r/B_r^*=0.52 in Figure 1), the entire discharge channel oscillates in unison and azimuthal perturbations (spokes) are either absent or negligible. Downstream azimuthally spaced probes show no signal delay between each other and are well correlated to the discharge current signal. In local mode (B_r/B_r^*=1.00, 1.48 in Figure 1), signals from azimuthally spaced probes exhibit a clear delay indicating the passage of "spokes" and are not well correlated to the discharge current. Spokes are localized oscillations propagating in the E×B direction that are typically 10-20% of the mean value; oscillations in global mode can be 100% of the mean value. The transition between global and local modes occurs at higher relative magnetic field strengths for higher mass flow rates or higher discharge voltages. Thrust is constant through mode transition but the thrust-to-power decreases by 25% due to increasing discharge current. Mode transitions provide valuable insight to thruster operation and suggest improved methods for thruster performance characterization.

References

[1] G. N. Tilinin, "High-frequency plasma waves in a Hall accelerator with an extended acceleration zone," *Soviet Physics-Technical Physics*, Aug. 1977.

[2] D. Brown and A. Gallimore, "Investigation of Low Discharge Current Voltage Hall Thruster Operating Modes and Ionization Processes," paper no. IEPC-2009-074, presented at the 31st International Electric Propulsion Conference, Ann Arbor, MI, 2009.

[3] M. J. Sekerak, R. R. Hofer, J. E. Polk, B. W. Longmier, A. Gallimore, and D. L. Brown, "Mode Transitions in Hall Effect Thrusters," 2013.

1-12

Temperature Dependence of Boron Doping Efficiency

S.N. Demlow [a], R. Rechenberg [b], M. Muehle [a,b], T.A. Grotjohn [a]

(a) Michigan State University, Electrical and Computer Eng., East Lansing, MI 48824, U.S.A.
(b) Fraunhofer USA Center for Coatings and Laser Applications, East Lansing, MI 48824, U.S.A.
(nicleysh@msu.edu)

Microwave Plasma Assisted Chemical Vapor Deposition (MPACVD) of semiconducting, boron-doped, single crystal diamond (SCD) has been an area of significant recent research interest. Due to its superlative properties, such as a wide bandgap, high breakdown voltage, and high electron and hole mobilities, diamond is a potentially exceptional semiconductor for electronic applications, especially high-temperature and high-power devices, such as vertical Schottky Barrier diodes. The realization of vertical diode structures requires the ability to reliably produce heavily doped (> 10^{20} cm^{-3}), free standing (> 500 μm thick) *p*-type substrates, however doping issues continue to be a limitation in this field. A problem of current interest in the growth of boron doped SCD is that of the decreasing doping efficiency at higher pressures (higher plasma discharge power) which has been noted by Achard *et al.* [1]. In our previous work [2] we have reported higher doping efficiencies than predicted by the model of Achard *et al*., and we theorized that it was due to a higher substrate temperature during the growth process. Work done on polycrystalline diamond films has shown that the diffusion coefficient of the boron dopant into the diamond lattice is dependent on the temperature of the substrate during growth by the Arrhenius equation [3]:

$$D = D_0 \exp(-E/kT)$$

Where D_0 is a constant, k is Boltzmann's constant, E (eV) is the thermal activation energy (i.e., diffusion barrier), and T is the growing temperature (K). As shown in the analysis in [3], the diffusion coefficient, D, at 1000°C (1.40×10^{-7} cm^2/s) is nearly twice the value at 700°C. It is therefore reasonable to assume that a similar temperature dependence relationship exists for boron doping in SCD, which will be more fully explored in this work.

We have previously demonstrated the effective characterization of boron-doped SCD, using non-destructive characterization methods such as Fourier-transformed infrared spectroscopy (FTIR) to investigate dopant concentrations from below 10^{17} cm^{-3} to over 10^{20} cm^{-3} [2]. This work expands upon our previous effort to grow and characterize high-quality diamond for electrical applications. Films are deposited on high pressure high temperature SCD substrates in MPACVD bell-jar reactor with plasma feedgas mixtures including hydrogen, methane, and diborane. We report on the results of growth experiments, and discuss the effect of the temperature of the substrate during growth on the plasma gas chemistry to solid-phase doping efficiency. We will also look at strategies for defect reduction, by characterizing the stress in the grown samples with X-Ray Diffraction, Raman spectroscopy, and Birefringence measurements.

References

[1] J. Achard, , F. Silva, R. Issaoui, O. Brinza, A. Tallaire, H. Schneider, K. Isoird, H. Ding, S. Koné, M. A. Pinault, F. Jomard, and A. Gicquel, Diam. and Rel. Mater., **20,** 145 (2011)
[2] S. N. Demlow, I. Berkun, M. Becker, T. Hogan, and T. A. Grotjohn, MRS Proc., **1395**, (2012)
[3]H. Li, T. Zhang, L. Li, X. Lü, B. Li, Z. Jin, and G. Zou, J. Crystal Growth, **312,** 1986 (2010)

1-13

Interaction of Atmospheric Pressure Dbds with Liquid Covered Tissues

Wei Tian [a] and Mark J. Kushner [b]

(a) Dept. of Nuclear Engr.& Radiological Science, University of Michigan, Ann Arbor, MI 48109, USA (bucktian@umich.edu)
(b) Dept. of Electrical Engr. & Computer Science, University of Michigan, Ann Arbor, MI 48109, USA (mjkush@umich.edu)

Atmospheric DBDs in contact with liquid are very important for tissue treatment in plasma medicine, from wound healing to disinfection. The tissues are rarely dry. Instead, they are often covered by a thin liquid layer, mostly water with dissolved gases and proteins, such as O_2 and alkane hydrocarbon (denoted as 'RH'). Although the liquid layers are typically 100s μm thick, they process radicals and ions produced in plasma prior their reaching the underlying tissue. In this presentation, we report on a computational investigation of DBDs in contact with a 200 μm thick liquid layer covering tissue. The model we used is *nonPDPSIM*, a 2-dimensional model in which Poisson's equation, electron temperature equation and transport equations for charged and neutral species are solved. The liquid layer is treated identically to gas as a partially ionized substance with higher density and designated permittivity. Water is allowed to evaporate into gas with a source given by its saturated vapor pressure. The rate of transport of gas phase species into the liquid is determined by Henry's law considerations. The reaction mechanism was mainly developed from the environmental science literature.[1]

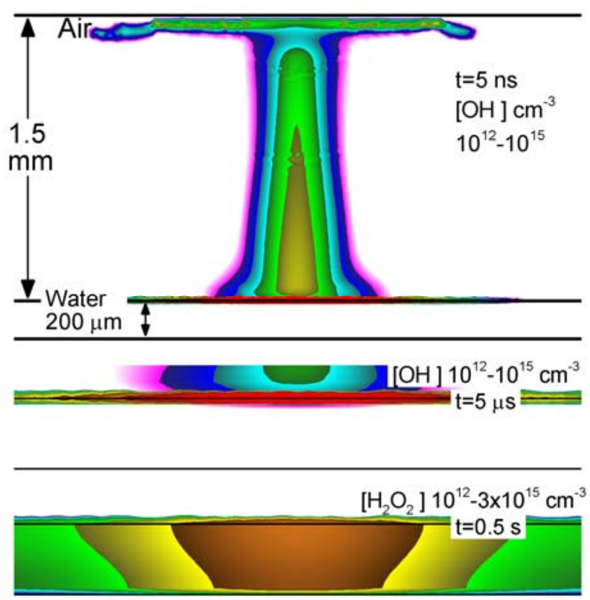

Figure 1 – Densities of OH and H_2O_2 in gas and liquid phase.

The DBDs are operated with multiple pulses of -15kV at 100 Hz followed by a 1 s afterglow. The hydroxyl radical and hydrogen peroxide are shown in Fig. 1. The majority of gas phase OH is produced directly above water in the water vapor layer. OH produced in the water is dominated by photodissociation during the plasma pulse and by OH diffusion during the afterglow. OH in the water rapidly produces H_2O_2, which is fairly unreactive and eventually reaches the tissue. In liquid water, the hydronium (H_3O^+) dominates the positive ions while O_2^- dominates the negative ions. The dominant RONS in the liquid are O_3, H_2O_2, and HOONO. For liquids containing RH, ROS are largely consumed, leaving R• (alkane radical) to reach the tissue.

References

[1] G. V. Buxton, C. L. Greenstock, W. P. Helman, A. Ross, J. Phys. Chem. Ref. Data. **17**, 513 (1988)

Work supported by NSF and DOE Office of Fusion Energy Science

An FMM-FFT Accelerated Hybrid Volume Surface Integral Equation Solver for Electromagnetic Analysis of Plasma-Engulfed Vehicles

Abdulkadir C. Yucel [a], Luis J. Gomez [a], Yang Liu [a], Hakan Bagci [b] and Eric Michielssen [a]

(a) Department of Electrical Engineering and Computer Science, University of Michigan, {acyucel, luisgo, liuyangz, emichiel}@umich.edu

(b) Division of Computer, Electrical, and Mathematical Sciences and Engineering, King Abdullah University of Science and Technology (hakan.bagci@kaust.edu.sa)

Space vehicles often are affected by communication blackout upon re-entering the Earth's atmosphere. The blackout arises when the vehicle interacts with the atmosphere around it, giving rise to dense plasmas that are impenetrable by electromagnetic waves. The vehicle itself often is covered in a thin and inhomogeneous plasma shell, the density of which decreases rapidly with distance from the vehicle surface. This plasma shell hinders the operation of antennas mounted on the side of the vehicle. As the vehicle moves through space, it also leaves behind a large plasma plume. This plume hinders the operation of antennas mounted on the back of the vehicle. The nature and density of the plasma shell and wake heavily depend on operational and environmental conditions and vary rapidly with the vehicle's position along its trajectory. To analyze the occurrence of communication blackout and facilitate the design of robust navigation systems, fast simulators capable of accurately characterizing the operation of antennas mounted on plasma-engulfed vehicles are called for.

The majority of past efforts aimed at analyzing antennas in plasma environments have relied on finite difference time domain solvers and were limited to relatively simple antennas and platforms [1]. Unfortunately they do not permit modeling of antennas on realistic structures. Recently a ray tracing technique was used to analyze antennas on plasma engulfed re-entry vehicles [2]. Albeit very powerful, this approach does not allow for a detailed modeling of the antennas and/or complex plasma structures that may arise in a turbulent wake.

In this study, a hybrid full-wave simulator that addresses the aforementioned challenges in analyzing scattering and radiation from plasma-engulfed space vehicles is proposed. The hybrid full-wave solver uses a surface integral equation solver to model the currents on the perfect electric conducting surface of the vehicle and a volume integral equation solver to model the electromagnetic fields in the plasma surrounding the vehicle. Both solvers were accelerated by a fast Fourier transform and fast multipole method (FMM-FFT) [3]. The hybrid solver uses a special block diagonal preconditioner for efficient and accurate characterization of scattering and radiation from plasma-engulfed space vehicles in highly inhomogeneous plasma distributions. Various computational results that demonstrate the efficiency, accuracy, and modeling versatility of this hybrid full-wave solver will be presented.

References

[1] M.D. White, Proc. IEEE Antennas Propagat. Soc. Int. Symp., 4B, 418-421, (2005).
[2] G. Vecchi et. al., Proc. IEEE Antennas Propagat. Soc. Int. Symp., 4, 181-184, (2004).
[3] J. M. Taboada et. al., IEEE Antennas Propag. Mag., **51**, 6, 20-28, (2009).

1-15

Phase Contrast Imaging and Characterization of X-rays Produced via Ultraintense Laser Plasma Interactions Using Coated Metallic Targets

Zhen Zhao, Thomas Batson, Bixue Hou, John Nees,

Alexander G.R. Thomas and Karl Krushelnick

Center for Ultrafast Optical Science,
University of Michigan
(zhen.zhao6@gmail.com)

Properties of hard X-rays generated via the interaction of an ultraintense laser with various solid targets were studied. A ~30 fs laser pulse operating at 0.5 kHz repetition rate was focused onto a ~1.5 µm spot, generating a focal intensity of ~10^{19} W/cm^2. The targets used were 85 mm diameter, ~12 mm thick Ni, Cu, Mo, Ag, and Sn. These metallic targets were coated with ~0.2 and ~1 um thick Al to study the effect of a low-resistivity coating on electron transport (and hence, X-ray generation) within the solid material. The X-ray source size was characterized by imaging a ~500 um thick GaAs knife edge with a cooled X-ray CCD camera. In addition, phase contrast imaging of a 3-D printed Michigan "M" (Fig. 1) was conducted using X-rays generated from Cu and Mo targets.

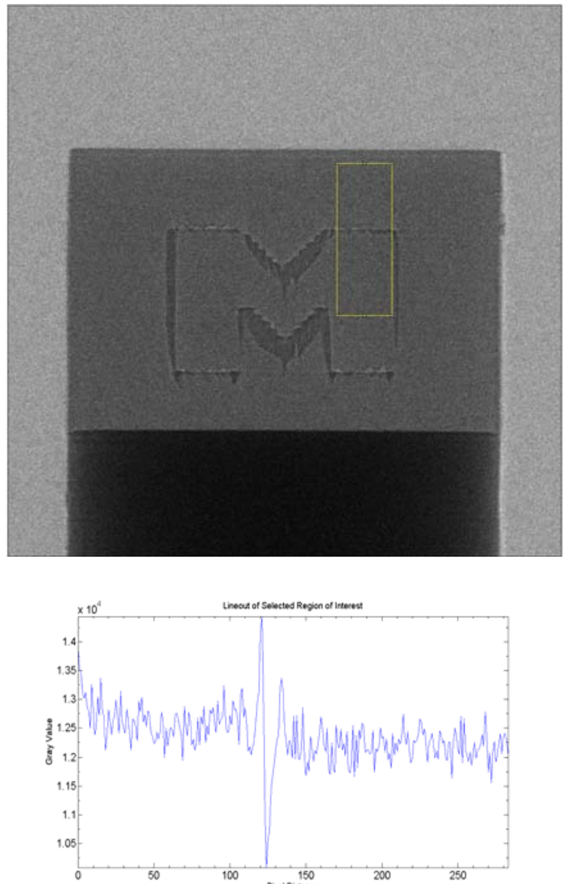

Figure 1 - (Top) X-ray image of a 3-D printed Michigan "M" using a Cu target with a compressed laser energy of ~5.5 mJ; (Bottom) Lineout of selected region of interest showing the characteristic pattern produced as a result of coherent interference from X-ray photons

References

[1] Kneip, S., APL, 093701, **99** (2011).
[2] Wilks, S.C., *et.al.,* PRL 69, **9** (1992).

Poster Session II

2-01

Film characterization of Agfa D7 and D8 x-ray film using a multiple anode x-ray source

J. S. Davis, R. P. Drake, P. A. Keiter, S. R. Klein, S. A. Bonhard, A. Cowherd, M. E. Darby

University of Michigan (davisjs@umich.edu)

X-ray radiographs are commonly used to determine the density of plasmas in many High Energy Density experiments. The important measure of the film is its ability to transmit light through the film after it has been processed. The “darkness” of the processed film is quantitatively known as the Optical Density (OD). The more the film is exposed to x-rays the darker the film and thus the higher the OD. If there is an HED plasma between the source and the film, the x-ray transmission through the plasma will be diminished and the density of the plasma can be calculated using the Beer- Lambert Law. Yet, even without a plasma the behavior of these films is highly dependent on various parameters of the x-rays used including photon energy, intensity, and angle of incidence. The standard for x-ray films was the Kodak direct exposure film (DEF) and this film’s response to x-rays was studied in depth by Henke et al in the 1980’s[1,2]. However, this film has been discontinued and new films namely the Agfa D7 and D8 films have begun to replace it and in order to be used to their fullest extent, they need to be characterized and calibrated as well. The goal of this work is to implement an x-ray source using either Copper or Chromium for the anode and a custom built spectrometer to act as a monochormator for the x-ray beam. The primary focus will be to calibrate the effects that varying the intensity and photon energy of the beam will have on the optical density of the film.

References

[1] B.L. Henke, S.L. Kwok, J.Y. Uejio, H.T Yamada, G.C. Young . J. Opt. Soc. Am. B. **Vol 1 No. 6**, 818(1984).
[2] B.L. Henke, F.G. Fujiwara, M.A. Tester, C.H. Dittmore, M.A. Palmer. J. Opt. Soc. Am. B. **Vol 1 No. 6**, 828(1984).

2-02

Simulations for the Elucidation of Electron Beam Properties in Laser-Wakefield Acceleration Experiments via Betatron and Synchrotron-Like Radiation

Paul G. Cummings and Alec G. R. Thomas

University of Michigan Center for Ultrafast Optical Sciences
(cummingp@umich.edu, agrt@umich.edu)

A promising application of laser-wake-field acceleration[1] (LWFA) technology is as a tunable source of x-ray and gamma radiation via synchrotron radiation. Such a source could have many potential applications, including microscale imaging of advanced composite materials[2]. Consequently, the generation of synchrotron radiation in LWFA experiments is investigated computationally using the particle-in-cell simulation code OSIRIS 2.0.

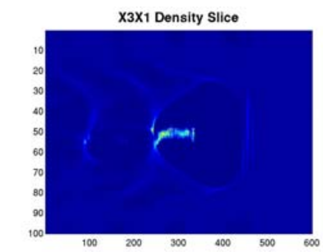

Figure 1: The first regime of radiation; the beam is still being accelerated, and is undergoing small-amplitude oscillations

In LWFA systems, electrons are accelerated by an electrostatic wake established by the laser pulse over a distance known as the dephasing length, L_d[1]. The fields in the wake are such that the beam naturally undergoes betatron oscillations while being accelerated. These oscillations can be broadly categorized into three regimes based on the beam propagation distance x. For $x < L_d$, the beam is being accelerated, and the betatron oscillations remain small. For $L_d < x < 2L_d$, the beam has passed the dephasing length and is now being decelerated by the wake, and the amplitude of the beam's betatron oscillations increases. Finally, when $2L_d < x$, the beam reenters the bulk plasma, and undergoes a hosing instability. The amplitude of the beam's betatron oscillations sharply increases at this point, until the beam breaks up.

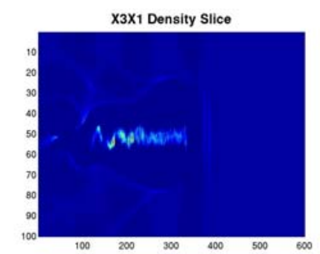

Figure 2: The second regime of radiation; the beam is being decelerated, and is undergoing larger-amplitude oscillations

Consequently, radiation emission in LWFA experiments can be controlled by varying the propagation distance of the laser pulse. Additionally, the emitted radiation properties could be used to assess the physical properties of the electron beam. For this work, the particle-in-cell code OSIRIS 2.0 was modified with a novel model for explicitly simulating synchrotron radiation, so these phenomena could be investigated computationally. A parameter sweep was performed, varying the propagation distance of the simulation from $0.75L_d$ to $4.0L_d$. The results from this parameter sweep are presented and discussed.

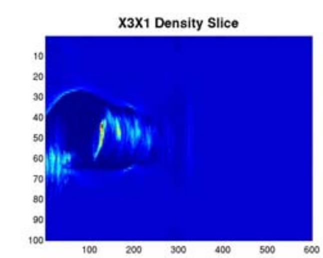

Figure 3: The third regime of radiation; the beam has entered the plasma and is undergoing a large-amplitude hosing instability.

References

[1] T. Tajima and J. M. Dawson, Phys. Rev. Lett. **43** 267 (1979)
[2] S. Kneip et al., Nat. Phys. **6** 980 (2010)

2-03

Multipactor Suppression via Secondary Modes in a Coaxial Cavity

Scott Rice and John Verboncoeur

Michigan State University Department of ECE (scott.a.rice@gmail.com, johnv@msu.edu)

Multipactor is a resonant phenomenon in which an electromagnetic field causes a free electron to impact a surface, resulting in the surface emitting one or more secondary electrons. If the surface geometry and electromagnetic fields are appropriately arranged, the secondary electrons can then be accelerated and again impact a surface in the bounding geometry. If the net number of secondary electrons participating in multipactor is nondecreasing, then the process can repeat indefinitely. This phenomenon is of considerable practical interest in the design and operation of high power resonant structures.

When the secondary electron yield (SEY) of a material is measured as a function of the incident electron kinetic energy, the curve follows a similar shape for many materials: At low incident kinetic energies, the SEY is low; at intermediate kinetic energies, the SEY is maximized at a material-dependent energy; at high kinetic energies, the SEY tapers down to zero with increasing energy. [1, 2] In order for multipactor to be self-sustaining, the average SEY over the multipactor path must be at least unity. This means that multipactor can only be sustained within a certain materialdependent range of incident electron kinetic energies.

This research investigates the feasibility of suppressing multipactor through the use of higher-order cavity modes which will modify the incident kinetic energy of the impacting electrons. Since the SEY is dependent upon the kinetic energy of the incident electron, our goal is modify the impacting electron velocities to reduce the average SEY to less than unity such that multipactor is not sustainable. Our previous work examined multipactor suppression in a coaxial geometry, in which the excitation and suppression modes were restricted to be TEM modes. The present research expands upon our previous work by examining the use of higher-order TE, TM, and TEM modes for suppression of multipactor in a notional coaxial cavity.

References

[1] Vaughan, "A New Formula for Secondary Emission Yield", IEEE Transactions on Electron Devices, Vol. 36, No. 9, September 1989, pp. 1963-1967, and revision "Secondary Emission Formulas", IEEE Transactions on Electron Devices, Vol. 40, No. 4, April 1993, p. 830.

[2] Furman and Pivi, "Probabilistic model for the simulation of secondary electron emission", Physical Review Special Topics – Accelerators and Beams, Vol. 5, No. 124404, 2002, pp. 124404-1 through 124404-18.

Work supported by U.S. Air Force Office of Scientific Research (AFOSR) grant on the Basic Physics of Distributed Plasma Discharges.

2-04

A Microdischarge Based Pressure Sensor

J. C. Wang, Z. Xiong, C. Eun, X. Luo, Y. Gianchandani, and M. J. Kushner

Univ. Michigan, Ann Arbor, MI 48109 USA (Junchwan@umich.edu, zxiong@umich.edu, eunc@eecs.umich.edu, xinluo@umich.edu, yogesh@umich.edu, mjkush@umich.edu)

Microscale pressure sensors having dimensions of 100's µm are often based on piezoresistive and capacitive methods. These techniques are challenged in harsh environments and at smaller sizes. Recently, a microplasma-based pressure sensor has been developed which is capable of dimensions at least an order of magnitude smaller. In these sensors, micro-plasmas are initiated between an anode and two competing cathodes in a sealed chamber filled with a rare gas mixture. A diaphragm attached to one electrode is deflected by external pressure which changes the inter-electrode spacing for one of the anode-cathode pairs, thereby redistributing the current collected by the two competing cathodes.

In this presentation, results from a computational investigation of the properties of microplasma-based pressure sensors will be discussed. The model used in this study, *nonPDPSIM*, solves Poisson's equation and transport equations for electric potential and charge densities; and electron energy conservation equation for electron temperature. Radiation transport is addressed using a Green's function approach. A Monte Carlo simulation is used to track sheath accelerated beam-like secondary electrons. The microplasma is sustained between an anode (A) and two grounded cathodes (K_1 and K_2) in a sealed chamber filled with 1 atm. Ar or rare gas mixtures. The anode is biased with hundreds of dc voltage. A reference cathode (K_1) is placed adjacent to the anode (A) while a sensing cathode (K_2) is mounted on the diaphragm separated by a gap of 10's µm. We find that following the electron avalanches between the edges of cathodes and anode induced by geometrically enhanced electric field current emission, a conductive microplasma is produced in the chamber within 10's ns. (See Fig. 1.) The current distribution on K_1 and K_2 varies with inter-electrode spacing (AK_2) between the anode (A) and sensing cathode (K_2) which is changed by deflection of the diaphragm by to external pressure. The current distribution can also be optimized by adjusting the impedance connected to electrodes.

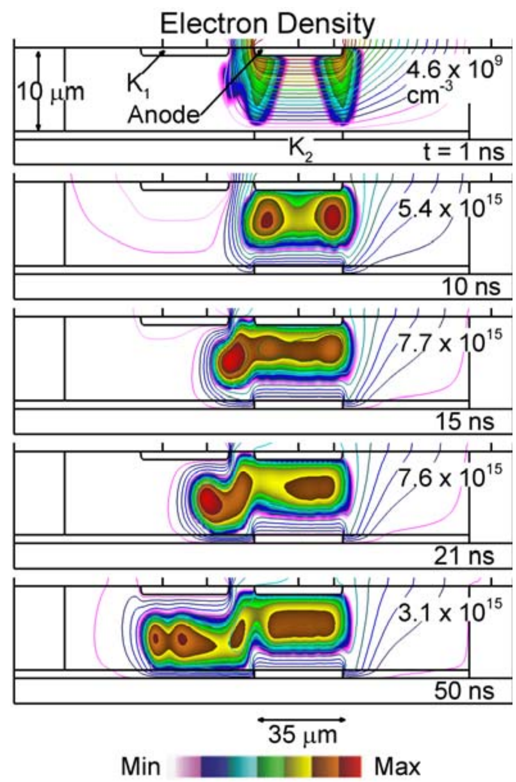

Figure 1 - Electron density (color Flood, cm^{-3}) and electric potential (contour lines, V) sustained in a sealed chamber filled with 1 atm of Ar.

Work was supported by the Advanced Energy Consortium

2-05

Description of the Sputtered Boron Atoms in the Plume of a SPT-70 Hall Thruster

Horatiu C. Dragnea and Iain D. Boyd

University of Michigan (horatiud@umich.edu, iainboyd@umich.edu)

Presently, the main failure mode of Hall thrusters is the erosion of the insulating channel walls. The expected thruster lifespan is determined by operating the thruster for a significant amount of time, generally much longer than the expected mission duration. This is inefficient and costly. Therefore a method that would determine the erosion rate and estimate the lifetime of the thruster without requiring extended operation times, would be of great interest. For this purpose, a non-intrusive cavity ring-down spectroscopy (CRDS) technique was developed by Lee et al. [1]. CRDS provides path integrated values of sputtered boron number density in the plume of the thruster. In order to characterize the entire flow field and estimate the erosion rate from the CRDS data, a computer simulation is developed. The research code MONACO [2], an implementation of the direct simulation Monte Carlo method [3], is used for this purpose. A new boundary condition type is developed in order to replicate the physics of boron sputtering.

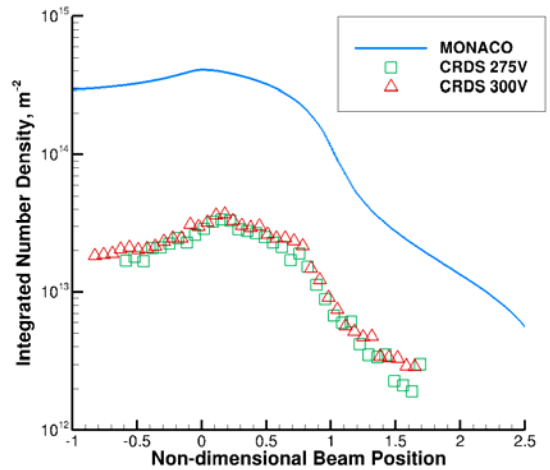

Figure 2- Comparison of MONACO and CRDS[1] results

The final results agree qualitatively, but the quantitative values disagree by an order of magnitude. The experimental values are lower than those obtained from MONACO, and this may be explained by the fact that the CRDS technique only detects the boron atoms in their ground electronic state. Hence atoms in higher electronic states are omitted, and so are boron atoms that become ionized. Including these additional effects would yield a higher and more realistic value of the erosion rate.

References

[1] Lee, B.C., Taylor, J.M., Leach, R.W., Yalin, A.P., and Gallimore, A.D. “Boron Nitride Erosio Measurements of an SPT-70 Hall Thruster via Cavity Ring-Down Spectroscopy,” Joint Army Navy NASA Air Force (to be published).

[2] Boyd, I. D., Van Gilder, D.B., and Liu, X. ”Monte Carlo Simulation of Neutral Xenon Flows in Electric Propulsion Devices,” Journal of Propulsion and Power, Vol. 14, No. 6, 1998, pp. 1009,1015.

[3] Bird, G. A., Molecular Gas Dynamics and the Direct Simulation of Gas Flows, Oxford Univ. Press, Oxford, England, UK, 1994

2-06

Modeling and Simulation of Strongly Coupled Plasmas

Mayur Jain, John Verboncoeur and Andrew Christlieb

Michigan State University (jainmayu@msu.edu, johnv@msu.edu, christli@msu.edu)

This work focuses on the development of new modeling and simulation tools for studying strongly coupled plasmas (SCP) as strongly coupled plasmas differ from traditional plasmas in that the potential energy is larger than the kinetic energy. A standard quasi neutral plasma approximation is inadequate in this case. In addition to the possibility of quantum effects, the standard quasi neutral plasma model does not account for two major effects in SCP: 1) the change in the permittivity for modeling electromagnetic waves and 2) the impact on relaxation of charged particles undergoing Coulomb collisions in a system with weakly shielded long range interactions. In this work we will focus on modeling and simulation of ultra cold plasmas, due to the nature of the experimental data being generated. This objective will be met through the development of: (i) electrostatic particle based models based on PIC and the Boundary integral Treecode (BIT) methods; (ii) electromagnetic particle based models based on PIC and new implicit particle methods based on treecodes; and (iii) the development of continuum models where long range correlation is incorporated thought fractional derivatives in time.

Developing Boundary Integral Treecode (BIT) models for ultra cold SCP: These mesh free methods offer advantages in simulating resolved SCP with boundary conditions, where a resolved PIC method will necessitate a prohibitively fine mesh when including boundary conditions for these systems. A treecode algorithm is employed to reduce the operation count from O(N2) to O(N log N). In this algorithm, the particles are divided into a hierarchy of clusters and the particle-particle interactions are replaced by particle-cluster interactions which are evaluated using multipole expansions. Barnes and Hut used monopole approximations and a divide-and-conquer evaluation strategy. Treecode algorithms have been very successful in particle simulations and there is ongoing interest in optimizing their performance.

Strongly Coupled Plasma Simulations with BIT: BIT, is an ideal method for studying strongly coupled electrostatic plasmas. Ultra cold plasmas only consist of 108 atoms. In this context BIT can be used to simulate a one to one representation of the ultra cold SCP, where each particle in the simulation represents a physical particle. BIT naturally resolves long range interactions.

References

[1] J.Barnes and P. Hut. A hierarchical o(nlogn) force-calculation algorithm. Nature 324,(1986)

[2] A.J. Christlieb, R. Krasny, J.P. Verboncoeur, J.W. Emhoff, and I.D. Boyd, Grid-free plasma simulation techniques, IEEE Transactions on Plasma Science 34 (2006).

[3] W. Dehnen, A hierarchical (n) force calculation algorithm, Journal of Computational Physics 179 (2002).

2-07

Control of Ion Energy & Angular Distribution in Dual-Frequency Capacitively Coupled Plasmas

Yiting Zhang and Mark. J. Kushner

University of Michigan
Electrical Engineering and Computer Science Department
Ann Arbor, MI 48109-2122 USA
(yitingz@umich.edu, mjkush@umich.edu)

Dual frequency capacitively coupled plasmas (DF-CCPs) provide the microelectronics fabrication industry flexible control, high selectivity and uniformity. The spatial variation of the phases, magnitude and wavelength of the high frequency (HF) rf bias will affect electron density, electron temperature, sheath thickness and ion transit time through the sheath. These variations ultimately affect the ion energy and angular distributions (IEADs) to the substrate, which are of critical importance for anisotropic etching or deposition. To optimize the separate control of rates of ionization and IEADs, the HF should be significantly different than the low frequency (LF), which results in the LF being few MHz. Although there are clear changes in the IEADs when varying the phase between the HF and LF, these changes are more modulations to the IEADs whose shape is dominated by the LF. However as the difference between the HF and LF becomes larger, the IEADs become more sensitive to the phase differences between the HF and LF, which provides an extra method to control and customize the IEADs.

In this paper, we report on a computational investigation of the rf power absorption, power coupling control and IEADs in an industry standard DF-CCPs. In this reactor, both the LF (2 MHz) and HF (up to 60 MHz) are applied to the lower electrode. The phase between the LF and HF is controlled. The Hybrid Plasma Equipment Module (HPEM) was employed to predict plasma properties and obtain the harmonic contributions of voltage waveforms applied to the same electrode. The operating conditions are 30 mTorr in pure Ar and $Ar/CF_4/O_2$ gas mixtures. The resulting IEADs are used as inputs to a feature profile model to assess etch profiles. The Profile simulations are used to demonstrate possible control schemes for over-etch through phase control.

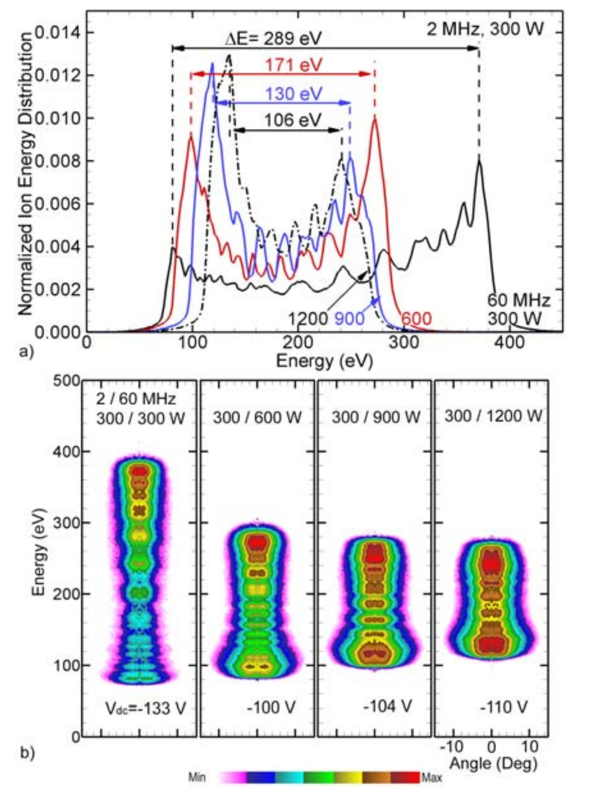

Figure 1 – Ion Energy Distribution (a) and Ion Energy and Angular Distribution (b) on the wafer in an Ar plasma at 30 mTorr. The low frequency 2 MHz power is fixed at 300 W with varying high frequency 60 MHz power from 300 W to 1200 W.

Work was supported by the Semiconductor Research Corp., NSF and LAM Research.

2-08

Statistical Analysis of the Geomagnetic Response to Different Solar Wind Drivers and the Dependence on Storm Intensity

R. M. Katus and M. W. Liemohn

AOSS, University of Michigan, Ann Arbor, MI, USA (rkatus@umich.edu, Liemohn@umich.edu)

The supersonic plasma from the Sun, the solar wind, streams past the Earth's magnetic field, creating a continuous low level of activity and occasionally causing near-Earth space storms. In this study, geomagnetic storms are investigated statistically with respect to the solar wind driver and the intensity of the event. The Hot Electron and Ion Drift integrator (HEIDI) model was used to simulate all of the intense storms (Dst_{min} < -100 nT) from solar cycle 23 (1996-2005). Four different configurations of HEIDI were used to investigate the outer boundary conditions and the electric field description. The storms are then classified as being a coronal mass ejection (CME) or corotation interaction region (CIR) driven events. The CME driven events are further sub grouped by the geoeffective structure responsible for the peak of the storm. The simulation results as well as solar wind and geomagnetic data sets are then analyzed along a normalized epoch timeline. The average behavior and model error of each storm type and the corresponding HEIDI configurations are then presented and discussed. The results are also examined as a function of the storm intensity and binned based on the magnitude of the minimum Dst. It is found that while the self-consistent electric field better reproduces stronger CME driven storms, the Volland-Stern electric field dose well reproducing the results for CIR driven events.

Investigating the Dependencies and Limitations of High Pressure Microwave Plasma Assisted Chemical Vapor Deposition of Single Crystalline Diamond

Matthias Muehle [a,b], M. F. Becker [a], T. Schuelke [a], J. Asmussen [a,b]

(a) Fraunhofer USA Inc. CCL, East Lansing, MI 48824, USA (mmuehle@fraunhofer.org)
(b) Michigan State University, East Lansing, MI 48824, USA

The high pressure, i. e. pressures > 150 torr, microwave plasma assisted chemical vapor deposition (MPACVD) of single crystal diamond (SCD) has been demonstrated [1]. Since then our research activities have focused on improving SCD growth rates and quality and also have been directed toward the development of microwave plasma reactors for high pressure diamond synthesis. Two new reactors, Reactor B [1] and Reactor C [2] have been developed. These reactors allow the safe and fast deposition of SCD material for pressures up to 300 Torr. However, the commercialization of an "electronic grade" SCD synthesis process requires the production of very high quality, large area SCD substrates at even higher growth rates. Increasing the SCD synthesis process pressure increases the growth rate [2.3] and also seems to enhance crystalline quality. Here a new reactor, Reactor B', is introduced, where a continuous wave (CW) microwave power supply is used. Past research performed with Reactor B used a pulsed 2.45 GHz power supply. At high pressures exciting Reactor B with a 120 Hz pulse rate causes a flickering plasma ball and the plasma becomes unstable, thus it limits the safe and low maintenance operation of the reactor to an upper pressure limit of 280 Torr. Using a CW power supply creates a homogenous and stable plasma and eliminates the upper pressure limitation 280 Torr .

The results of a number of exploratory experiments using reactor B' are presented and a newly defined stable and safe operational range for Reactor B' is presented. The growth rate as a function of the pressure for varying methane concentrations is analyzed. For a methane concentration of 5% a linear increase versus pressure is observed. This is the same behavior as previously observed [2]. At 400 Torr the hydrogen plasma remains stable, however vortex formation in the presence of methane plasma occurs making the plasma instable. Thus, the safe operational range has been defined up to 380 Torr. For higher pressures either a new set of parameters must be investigated or a new reactor design must be introduced. Additionally the dependency of the growth rate as a function of methane concentration is analyzed. For low concentrations a linear behavior has been identified, at higher methane concentrations (> 6-7%) the growth rate flattens out and appears to saturate versus additional increases of methane.

High quality diamond samples are grown at 380 Torr without nitrogen addition in the gas phase. Optical absorption spectroscopy of the diamond displays the high crystalline quality. The absorption behavior is outstanding and is similar to or even better that the samples that have been grown previously in Reactors A, B and C. Based on the optical absorption the nitrogen concentration in the synthesized SCD appears to be below 100 ppb. Birefringence imaging shows a still detectable amount of internal crystalline stress. Initial exploratory experiments using Reactor B' operating in the 300-400 torr process regime indicate that SCD is synthesized with the highest crystalline quality and with growth rates of ~ 20 μm/hour.

References

[1] Y-S Yan, et al., Proc. Nat. Acad. Sci. 99, 12523-12525, (2012).
[2] J. Lu, et.al Diamond and Related Materials **37**, 17 - 28 (2013).
[3] Y. Gu, et al. Diamond and Related Materials **24**, 210 - 214 (2012),
[4] S. Taylor and P. Pix, J. Appl. Phys. **101**, 2389 (2009).

Adaptively Matched Dual Band GPS Antenna for Variable Plasma Environments

Xiuzhang Cai, Eric Michielssen, Xiaoying Gu and Amir Mortazawi

Dept. of Electrical Engineering and Computer Science, University of Michigan (caixz@umich.edu, emichiel@umich.edu, markgu@umich.edu, amirm@eecs.umich.edu)

Hypersonic vehicles oftentimes experience diminished electromagnetic communication and sensing capabilities due to dense plasma that forms around the vehicle during re-entry. During so-called blackout, this plasma prevents all communication to the vehicle, which now must navigate entirely using inertial motion sensors. Unfortunately, these sensors are incapable of accurately predicting vehicle position and orientation for extended periods of time. Therefore antennas that are insensitive to plasma loading are key to enhancing navigational accuracy.

This paper considers the design of a novel dual (L1 + L2) band GPS antenna for variable plasma environments experienced by hypersonic vehicles during re-entry. Traditional GPS patch antennas use a single feed and asymetric patch arrangements to achieve right hand circular polarization; while very compact they also exhibit a narrow polarization/axial ratio (AR) and impedance bandwidths. When operating in a plasma enviroment, these antennas' performance is affected by (i) signal loss / attenuation through the plasma layer, (ii) polarization mismatch [1] and (iii) impedance mismatch [2]; (ii) and (iii) further reduce the antenna's operational bandwidth. While little can be done to reduce signal loss, proper design of the antenna may mitigate (ii) and (iii).

Here we propose a novel double-feed dual band GPS antenna with AR bandwidth exceeding 100 MHz in both the L1 and L2 bands, thereby rendering making the antenna polarization highly insensitive to plasma loading. The two feeds capacitively couple to two stacked cavity-backed patches that are separated from the plasma via a carefully designed radome. To achieve acceptable impedance bandwidth, a tunable matching network with a feedback system is called for. Here, an LC matching network is realized using varactor (capacitor) diodes that improves the antenna return loss from -5dB to -20dB for variable plasma conditions experienced by a typical re-entry vehicle. The feedback system is composed of a single band transmitting antenna, a return loss measurement system, and a controller. The return loss measured by this transmitting antenna is used to approximately characterize the plasma environment and to estimate the antenna impedance; the controller then sets the proper bias voltage to the varactors to (approximately) match the GPS antenna.

References

[1] Z.H. Qian, R.S. Chen, K.W. Leung, et al. Progress Electromagn Res 52(2005).
[2] L. Zhao, B. W. Bai, W. M. Bao, and X. P. Li, Int. J. of Antennas Propag. (2013) 823626

Development of a Compact Pulse Generator for X-Ray Backlighting of Planar Foil Ablation Experiments

D.A. Yager-Elorriaga, A.M. Steiner, S. Patel, R.M. Gilgenbach, Y.Y. Lau, and N.M. Jordan

University of Michigan (dyager@umich.edu)

A 70 kV, 60 kA compact pulse generator (0.7m x 0.9m x 0.3m) has been constructed and successfully tested with a resistive load using a Linear Transformer Driver (LTD) capacitor-switch configuration. The generator consists of 6 bricks connected in parallel, where each brick contains two oppositely charged capacitors (+/-70kV, 40nF) and a low inductance L-3 spark-gap switch (93nH). The bricks are connected to the load through a parallel plate transmission line. The generator is designed to drive a hybrid x-pinch to serve as a diagnostic for planar foil ablation experiments on the 1-MA LTD at the Michigan Accelerator for Inductive Z-pinch Experiments (MAIZE) facility.[1,2] The hybrid x-pinch diagnostic consists of a 10-50μm Al, Mo, or W wire between two conical tungsten electrodes and will be used as a backlighter in addition to the current 775nm Ti:sapphire laser. Testing of the x-pinch load is currently underway. In addition, the generator may be used to create external magnetic fields for magneto Rayleigh-Taylor (MRT) experiments on the 1-MA LTD. Preliminary results of generator characterization will be presented.

References

[1] J. C. Zier, R. M. Gilgenbach, D. A. Chalenski, Y. Y. Lau, et al, Phys. Plasmas **19**, 032701 (2012).
[2] Jacob Zier, “Ablation Dynamics and Instabilities of Metallic Plasmas generated using MA-Scale Current Drivers”, Ph.D. Dissertation, University of Michigan, (2011).

This work was supported by DoE Award number DE-SC0002590, NSF Grant number PHY 0903340, and by US DoE through Sandia National Labs award numbers 240985, 767581 and 768225 to the University of Michigan. This material is also based upon D.A. Yager-Elorriaga’s work supported by the National Science Foundation Graduate Student Research Fellowship under Grant No. DGE 1256260. S. G. Patel and A. Steiner were supported by NPSC fellowships through Sandia National Laboratories.

Electrical Contacts: A Voltage Scale for Thermal Runaway and Issues in Measurements of Constriction Resistance

Peng Zhang [a], Y. Y. Lau [a], D. Chernin [b] and R. M. Gilgenbach [a]

(a) Department of Nuclear Engineering and Radiological Sciences, University of Michigan, Ann Arbor, MI 48109-2104
(b) Science Applications International Corporation, McLean, VA 22102, USA

Contact problems account for 40 percent of all electrical/electronic failures. Severe heating due to local current crowding at thin film contacts [1] and at bulk contacts [2] is also a concern to high power microwave sources, pulsed power systems, field emitters, thin film devices and integrated circuits, and interconnects, etc. Here, we investigate electro-thermal instability (ET) due to the increase in electrical conductivity as temperature increases, which may lead to thermal runaway at fixed voltage. We deduce a voltage scale for ET onset [3], $V_s = \sqrt{\kappa / \sigma_0'}$ [in volts], where κ is the thermal conductivity [in W/(m-K)] and σ_0' is the rate of change of the electrical conductivity with respect to temperature [in 1/(ohm-m-K)]. V_s depends only on material properties and is independent of geometry or the operating voltage. It measures the intrinsic tolerance of the material to ET. The calculated V_s are listed for several common materials, Si, Ge, C (graphite), and SiC [3], as shown in Table 1. We conclude that SiC is the most resistant to thermal runaway for the same geometry and the same operating voltage, consistent with the well-known property of this material.

Table 1. Voltage scale for electro-thermal runaway

	κ [W/(m-K)]	σ_0' [1/(Ω-m-K)]	V_s [Volt]
Si	142	0.0012-0.7	14.2-348.9
Ge	58	0.0001-0.05	34-761.6
C (graphite)	127	1.67×10^{-4}-8.33×10^{-6}	872.9-3903.8
SiC	370	4×10^{-7} or negative	3×10^{4}

The paper also addresses some intrinsic difficulties in experimental measurements of the contact (constriction) resistance. The potential sources of error are identified. We compare the evaluation of spreading resistance from our exact theory with evaluations from recent computer simulations and with results from recent experimental measurements [4].

References

[1] P. Zhang et. al., J. Phys. D: Appl. Phys. 46, 065502 (2013); Corrigendum, ibid, vol. 46, p. 209501 (2013); IEEE J. Electron Devices Soc., 1, 83 (2013).
[2] P. Zhang, doctoral dissertation, U Michigan, Ann Arbor (2012).
[3] Y. Y. Lau, et. al., IEEE PPPS Conference Proceedings (June 2013).
[4] P. Zhang, et al., IEEE Holm Conference Proceedings (September 2013).

Work supported by an AFOSR grant FA9550-09-1-0662, and L-3.

2-13

Finite Difference Weighted Essentially Non-Oscillatory Schemes with Constrained Transport for Ideal Magnetohydrodynamics

Qi Tang [a], Andrew Christlieb [a] and James Rossmanith [b]

(a) Department of Mathematics, Michigan State University (tangqi@msu.edu)
(b) Department of Mathematics, Iowa State University

Numerical methods for solving the ideal magnetohydrodynamic (MHD) equations in more than one space dimension must confront the challenge of controlling errors in the discrete divergence of the magnetic field. The constrained transport (CT) schemes have been shown successful in stabilizing MHD computations. During the evolution steps in a CT scheme, a magnetic field value is first predicted by a method that does not exactly preserve the divergence-free condition, followed by a correction step that controls these divergence errors numerically.

Our goal is to discover a high-order adaptive MHD solver through CT methods and AMR technique. In this presentation, we will introduce a class of high-order finite difference unstaggered CT schemes for solving ideal MHD systems on a Cartesian mesh. In particular, we mainly focus on the following most important properties of our schemes: (1) all quantities, including all components of the magnetic field and magnetic potential, are treated as point values at cell edges; (2) the spatial and temporal order of accuracy are both increased to 4th-order; (3) no multidimensional reconstructions are needed in any step; (4) we develop a class of high-order finite difference schemes via WENO idea for evolving the magnetic potentials in both 2D and 3D. Several 2D and 3D numerical examples are presented to show high-resolution and essentially no oscillations for test problems with shocks and discontinuities developed in the solutions.

References

[1] J. Rossmanith, SISC. **28** 1766 (2006)
[2] H. Christiane, J. Rossmanith and B. Taetz JCP. **230** 3803 (2011)
[3] H. Christiane, J. Rossmanith and B. Taetz SISC. **35** A623 (2013)
[4] C. Shen, J.M. Qiu and A. Christlieb, J. Comp. Phys. 230 3780 (2011)

3-01

Preliminary Investigation of the High-energy X-ray Spectrum of Pinhole Point Projection Backlighters

Jeff Fein [a], P.A. Keiter [a], C.C. Kuranz [a], C.M. Krauland [a], J. Peebles [b], L.C. Jarrott [b], S.R. Klein [a], J. Davis[a], R. Gillespie [a], J.P. Holloway [a], R.P. Drake [a], D.D. Meyerhofer [c]

(a) University of Michigan, Ann Arbor, MI 48105 (jrfein@umich.edu)
(b) University of California, San Diego, San Diego, CA
(c) University of Rochester, Rochester, NY

Laser-produced hot electrons may present many undesirable effects in high-energy-density physics experiments. In particular, the secondary production of high-energy x-rays creates a background that reduces the signal-to-noise. Experiments were performed to study the hot electron-induced high-energy x-ray background present in pinhole point-projection x-ray backlighters. In these experiments, bremsstrahlung x-ray spectrometers (BMXS[1]) were used to measure the high-energy x-ray signal from the backlighter targets. The response of the BMXS diagnostic is capable of retrieving both the continuous x-ray spectrum and a best fit of the hot electron temperature describing the hot electron energy distribution. We present a preliminary analysis on how the x-ray spectra depend on backlighter and pinhole substrate material. Additionally, we will discuss the x-ray spectra angular dependence.

References

[1] Chen, C. D., et al. A Bremsstrahlung spectrometer using k-edge and differential filters with image plate dosimeters. Rev. Sci. Instr., 79(10), (2008)
[2] Krauland, C. M., et al. An evaluation of high energy bremsstrahlung background in point-projection x-ray radiography experiments. The Review of scientific instruments, 83(10), (2012)

Direct Control of Electron Beam from a Laser Plasma Accelerator Using Adaptive Optics with a Genetic Algorithm

Zhaohan He [a], Vivien Lebailly [b], Bixue Hou [a], John Nees [a], Karl Krushelnick [a] and Alec Thomas [a]

(a) Center for Ultrafast Optical Science, University of Michigan, MI 48109
(b) Polytech Paris-Sud - Université Paris-Sud, Orsay, France

A deformable mirror (DM) is used as adaptive optics in a laser wakefield accelerator (LWFA) to manipulate the laser produced electron beam parameters including the charge distribution, beam direction, beam divergence and energy distribution. Collimated electron beams in the 100 keV energy range are produced in a high-repetition-rate LWFA [1]. The experiments were performed on the Lambda Cubed Laser at CUOS - a tabletop sub-TW laser system capable of delivering 10 mJ, 35-fs pulses at a central wavelength of 790 nm. The laser beam is focused by an off-axis parabolic mirror to a spot size of 2.5 μm, and interacts with an argon gas plume generated from a 100 μm diameter orifice. Electrons are detected 35 cm from the source with a scintillator screen (FOS by Hamamatsu) with a lens-coupled CCD camera. The deformable mirror has been originally used to correct wavefront distortions in the system for achieving near diffraction-limited focusing [2]. The photodiode signal of second harmonic generation in a barium borate crystal is used as a figure of merit for searching the best optimal DM configuration in a genetic algorithm. We modified the algorithm such that the electron image acquired by the CCD camera can be used to provide figures of merit to change the mirror shape for direct control of electron beam properties. For example, the charge distribution and beam direction can be manipulated by the DM. Additionally, a magnet electron spectrometer can be incorporated so that the energy distribution of the electrons can provide direct feedback for the algorithm. The effectiveness and limitation of this technique will be discussed.

References

[1] Z.-H. He, B. Hou, J. A. Nees, J. H. Easter, J. Faure, K. Krushelnick and A. G. R. Thomas, New J. Phys. **15**, 053016 (2013).

[2] O. Albert, H. Wang, D. Liu, Z. Chang, and G. Mourou, Opt. Lett. **25**, 1125-1127 (2000).

3-03

Quasi-Classical Study of Atomic States

Gautham Dharuman [a], John Verboncoeur [a] and Andrew Christlieb [b]

(a) Dept. of Electrical Engineering, Michigan State University (dharuman@egr.msu.edu, johnv@msu.edu)
(b) Dept. of Mathematics, Michigan State University (christlieb@math.msu.edu)

Quasi-classical treatment was adopted for studying atomic structure to decrease the computational expense which is usually high in case of a complete quantum mechanical treatment of many-electron atoms. The quantum effects are realized in a classical model by introducing momentum dependent pseudo-potentials corresponding to the Heisenberg Uncertainty Principle and the Pauli Exclusion Principle [1]. These potentials exclude the regions of phase space forbidden by these principles.

Determining the states of an N-electron atom begins with constructing the classical Hamiltonian modified to include the Heisenberg pseudo-potential for each electron to prevent their collapse into the nucleus and the Pauli pseudo-potential for electrons with like spins to prevent their presence in similar states. Ground state of the atom is obtained by finding the global minimum of the high dimensional energy surface spanned by 6N variables of the Hamiltonian. BFGS-quasi Newton method adopted in [1] was used for the optimization. However, this method can fail to converge to the global minimum if the initial guess of the variables is not close enough to the ground state configuration. A crucial step in the method is the 'line search' which is a sub-minimization problem involving determination of an optimum step size for updating the variables along a search direction. In case of smooth functions usual methods adopted for this step involve interpolation using a quadratic/cubic polynomial which could be expensive and slow [2]. To overcome these constraints, a Quasi-Monte Carlo (QMC) brute-force method [3] involving Quasi-Random Numbers (QRNs) was implemented. This method does not involve derivatives and can function without any assumption of exact initial values for the variables. In comparison to random numbers, QRNs have a uniform distribution due to their low discrepancy which is a required property for capturing minima while sampling the energy surface. A Halton sequence [3] of QRNs formed the basis of this scheme. Preliminary results of this study involving H, He, Li and C atoms are listed in Table 1. Ground state energies (in atomic units) calculated using the BFGS and QMC schemes are compared with the accurate Hartree-Fock (HF) results [4]. It is evident that the model and the minimization schemes require further improvement. Excited states, in particular the metastable states which constitute the local minima of the energy surface, could be effectively located using a hybrid BFGS-QMC scheme. Improvement of the individual schemes and determination of the excited energy levels of low atomic number elements is the focus of ongoing research.

Element	HF(a.u.)	BFGS(a.u.)	QMC(a.u.)
H	-0.5	-0.5	-0.4999
He	-2.8617	-3.0623	-3.0621
Li	-7.4327	-8.0375	-7.8272
C	-37.6886	-44.1553	-38.8051

Table 1 – List of ground state energy values of H, He, Li and C atoms calculated using the BFGS and QMC schemes and the accurate results from HF

References

[1] J. S. Cohen, Phys. Rev. A **51**, 266 (1995).
[2] R. Fletcher, *Practical Methods of Optimization,* John Wiley and Sons (1987).
[3] H. Niederreter and K. McCurley, Computing **22**, 119 (1979).
[4] C. F. Bunge et al., Phys. Rev. A **46**, 3691 (1992)

3-04

Effects of Random Circuit Fabrication Errors on Small Signal Gain and Output Phase in a Traveling Wave Tube

I. M. Rittersdorf [a], T. M. Antonsen, Jr. [b], D. Chernin [c], and Y. Y. Lau [a]

(a) University of Michigan (ianrit@umich.edu)
(b) University of Maryland
(c) Science Applications International Corporation

Traveling-wave tubes (TWTs) are widely used as amplifiers in broadband radar, communications, and electronic warfare [1]. Random fabrication errors in the manufacture of slow wave circuits may have detrimental effects on the performance of traveling-wave tubes of all types. Such errors will pose an increasingly serious problem as TWTs are designed and built to operate in the sub-millimeter wavelength regime, which employ miniature, difficult-to-manufacture slow-wave circuits. As a result of performance degradation from random errors, the manufacturing yield, and therefore the cost of manufacturing, is seriously affected. Analytical and numerical results on the expected degradation of the small signal gain, and the expected output phase variations, of a TWT when small random, axially varying perturbations are present in the circuit phase velocity are obtained (Fig. 1). A scaling law for the ensemble-averaged gain and phase variations is derived. The present work accounts for non-synchronous beam velocities and the inclusion of Pierce's "space charge" effects [2]. In the absence of space charge, analytical results using a perturbative approach and a Ricatti method compare favorably with numerical integration of the governing equation using 5000 random samples, in both gain and phase modifications as a result of the errors in the phase velocity that are randomly distributed along the slow wave circuit (Fig. 1). Results on the effects of non-synchronous beam velocities and of ac space charge are reported. Effects of internal reflections are investigated [3]. This work was supported by AFOSR, L-3, Northrop Grumman, and MIPSE.

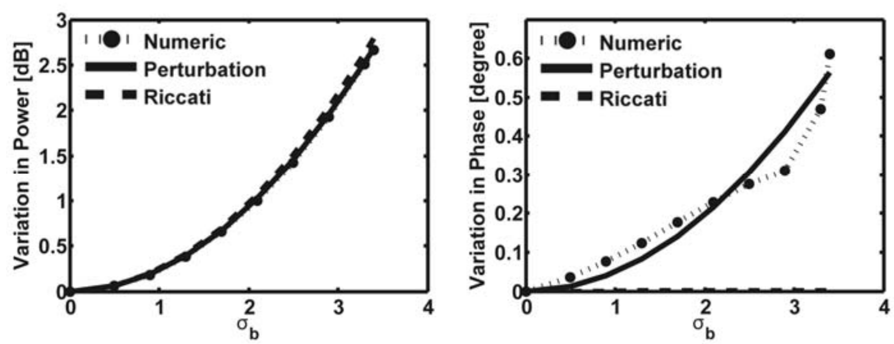

Figure 1 - Mean values of the power (left) and phase (right) phase at a TWT output relative to the unperturbed values, as a function of circuit random errors, from three approaches.

References

[1] P. Pengvanich, D. Chernin, Y. Y. Lau, J. W. Luginsland, and R. M. Gilgenbach, *IEEE Trans. Electron Devices* **55**, 916 (2008); and references therein.

[2] I. Rittersdorf, T. M. Antonsen, Jr., D. Chernin, and Y. Y. Lau, *IEEE J. Electron Devices Society* (In The Press, 2013).

[3] D. Chernin, I. Rittersdorf, Y. Y. Lau, T. M. Antonsen, Jr., and B. Levush, *IEEE Trans. Electron Devices* **59**, 1542 (2012).

3-05

Studying Miniature Electrodynamic Tethers and Interaction with the Low Earth Orbit Plasma

Iverson C. Bell and Brian E. Gilchrist

The University of Michigan, Ann Arbor, MI 48109 (icbell@umich.edu)

The sub-kilogram, "smartphone"-sized satellite is a transformative concept, inspired by the success of nanospacecraft (1–10 kg) and millimeter-scale wireless sensor network concepts. These ultra-small satellites, known as picosatellites (100 g–1 kg) and femtosatellites (<100 g), show potential to be less costly to manufacture and boost into orbit. Thus, it may be possible to launch them in large numbers, enabling unique capabilities. The result is that highly capable, cost-effective ultra-small spacecraft ("satellite-on-a-chip" or "ChipSat") as well as a "constellation" of spacecraft for multipoint, simultaneous thermospheric/ionosphere science and potentially for Earth Systems studies are being seriously considered. [1-3]

Organized "fleets" of pico- or femtosatellites, however, will need a high level of coordination and maneuverability capability (i.e., propulsion). Also, many of these satellites can have a high area-to-mass ratio, which results in a short orbital lifetime in low Earth orbit due to atmospheric drag.

We summarize studies that found that short (few meters), semi-rigid electrodynamic tethers can provide 10-g to 1-kg satellites with complete drag cancellation and the ability to change orbit. We also present progress on the Miniature Tether Electrodynamics Experiment (MiTEE), currently in development. The goal of MiTEE will be to demonstrate miniature electrodynamic tether capabilities in space and study the fundamental dynamics and electrodynamics of the propulsion system.

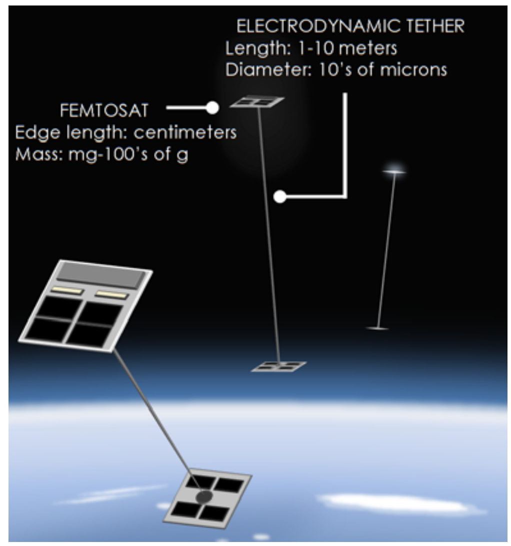

Figure 1 - Concept of ED tethers with pairs of femtosats as a maneuverable, coordinated fleet.

To enhance our understanding of the feasibility of the propulsion concept, we have been investigating plasma contactors. Electron emitting and collecting plasma contactors are critical because they close the tether circuit in the ambient plasma, allowing current to be conducted in the tether. In previous trade studies, we made several simplifying assumptions to estimate current. Our goal in this poster is to improve our current collection estimate by presenting progress made on ground-based plasma experiments that capture critical characteristics of the LEO environment, like the ratio of the Debye length to the ChipSat dimension.

References

[1] R.L. Balthazor, et al., Aerospace Conference, 2009 IEEE (2009).

[2] P.P. Sundaramoorthy, E.K.A. Gill, and C.J.M. Verhoeven, 61st International Astronautical Congress (2010).

[3] J. Bouwmeester and J. Guo, Acta Astronautica. **67**. (2010).

3-06

Atmospheric Pressure Microwave-Powered Microplasma Source Based on Strip-Line-Like Structure

P. Liu and T. A. Grotjohn

Michigan State University, East Lansing, MI 48824 USA

Portable low cost microplasma sources received great interest in the past decade due to their widely various application such as materials processing, biomedical, and chemical analysis and optical radiation sources.[1-6] Especially, for the atmospheric pressure microwave plasmas, without the requirement of vacuum systems, it is easily to realize 3D operations and also portable low-cost become easy to achieve. Further, by using higher frequency energy (radio frequency and microwave) to power the microplasma discharge, non-LTE (non-local thermo-dynamic equilibrium) cold plasma which comparing with other traditional high pressure plasma has the great advantages such as reducing the erosion of electrodes and producing high power density plasma with lower power consumption.

In this investigation a microwave powered microplasma system based on a double-strip-line structure is developed for the generation of atmospheric pressures plasmas with various feed-gases and feed-gas mixtures. The microplasma system is constructed with the top and bottom copper strip-lines separated by a dielectric material. The strip-line structure powered at one end and the plasma formed at the other end where the two copper strip-lines are brought together to a gap with 250 microns separation. The feed-gas is flowed through a channel in the dielectric such that it exits with the feed-gas flowing into the gap created by the two strip-lines. The gas flow channel in the dielectric is 250 microns high by a quarter inches wide. The flow rate is varied from 900-2400 sccm.

Argon, argon-oxygen and argon-helium microplasma discharges are formed in the gap between the two copper strip-lines. In argon-oxygen plasma, oxygen percentage varied from 1% up to 5%. In argon-helium plasma, helium percentage varied from 10% to 90 %. The microwave power used for the discharges varies from 5 to 60 Watts. Micro-camera was used to take pictures of the plasma to show the shapes and intensities of the microplasma outside the gas-channel. Optical emission spectroscopy technique was used to diagnose the discharges. The existence and variation of concentration of high energy level species are identified and measured, and their variations with different input power gases percentages are discussed. Other properties of the microplasma such as gas temperatures and electron temperatures are also measured. Some applications such as etching of single/poly-crystalline diamond are also performed.

References

[1] J. Kim, and K. Terashima, Appl. Phys. Lett. 86 (2005) 191504
[2] J. Kim, M. Katsurai, D. Kim and H. Ohsaki, Appl. Phys. 93 (2008) 191594
[3] K. Ogata and K. Terashima, J. Appl. Phys., 106(2009) 023301
[4] J. Gregorio, L. L. Alves, O. Leroy, and C. Boisse-Laporte, Eur. Phys. J. D., 50(2010) 627
[5] S. Schermer, N. H. Bings, A. M. Bilgic, R. Stonies, E. Voges. J. A. C. Broekaert, Spectrochimica Acta Part B 58 (2003) 1585-1596
[6] U. Engel, A. M. Bilgic, O. Haase, E. Voges, and J. A. C. Broekaert, Anal. Chem. 72(2000) 193

3-07

Supersonic, Single-mode, Shockwave-driven Kelvin-Helmholtz Instability Experiment on OMEGA-EP

W.C. Wan [a], G. Malamud [a b], C.A. Di Stefano [a], C.C. Kuranz [a], A. Shimony [b], R.P. Drake [a]

(a) Department of Atmospheric, Oceanic, and Space Sciences, University of Michigan, USA (wwan@umich.edu)

(b) Department of Physics, Nuclear Research Center, Israel (guy.malamud@gmail.com)

Hydrodynamic instabilities are commonly encountered in a variety of high-energy-density systems, including fusion experiments and various astrophysical processes. Shear flow at a fluid interface gives rise to the Kelvin-Helmholtz instability, which then results in mixing between the layers. This poster will address the theory[1], data, and preliminary analysis of a recent experiment performed at the OMEGA-EP facility that studied the dampening of the Kelvin-Helmholtz instability as a result of compressibility effects in a high convective Mach number regime. A laser-driven shockwave was used to generate a sustained shear flow between a low-density foam and high-density plastic. The instability growth was assisted by seeded, single-mode perturbations of varied wavelengths. Our primary diagnostic was an x-ray radiography technique known as Spherical Crystal Imaging.

This work is funded by the NNSA-DS and SC-OFES Joint Program in High-Energy-Density Laboratory Plasmas, grant number DE-FG52-09NA29548, and by the National Laser User Facility Program, grant number DE-NA0000850, with additional support provided under Cooperative Agreement No. DE-FC52-08NA28302 through the Laboratory for Laser Energetics, University of Rochester.

References

[1] G. Malamud et al., High Energy Density Physics. **9,** 4 (2013)

Microwave Excited Microplasmas at Low Pressure as a Vuv Photon Source

Peng Tian and Mark J. Kushner

Dept. of Electrical Engineering and Computer Science
University of Michigan, Ann Arbor, MI, 48109, USA
(tianpeng@umich.edu, mjkush@umich.edu)

Microplasmas in rare gases and rare gases mixtures can provide efficient and discretely tunable sources of UV/VUV light. Such small inexpensive UV/VUV light source can be implemented in many applications ranging from analytical chemistry, mass spectrometry and surface analysis. In particular, microwave excited microplasma sources can provide some tangible benefits compared to direct current (DC) microplasmas, such as lower excitation voltage, high power efficiency and smaller sheath voltage which prolongs the life time of the device. A microwave excited microplasma sources excited by a split-ring resonator (SRR) antenna in rare gas mixtures operated in ceramic cavities with sub-mm dimensions have been developed as discretely tunable VUV source for chemical analysis. Controlling wavelengths and the ratio of ion to VUV fluxes are important to achieving chemical selectivity.

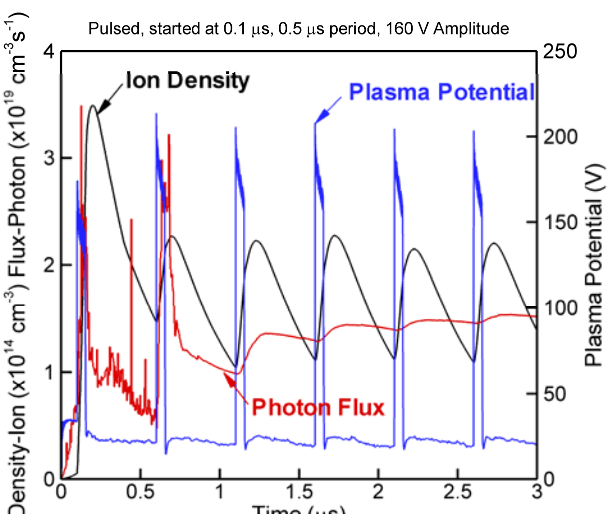

Figure 1 – Ion Density, Photon Flux and Plasma Potential in a Pulsed Microplasma.

In this project, the SRR microwave plasma light source will be investigated using a plasma hydrodynamics model where the electron energy distribution and radiation transport are address by Mote Carlo simulations. The plasma is excited by a 2.5 GHz power at pressures of 1-tens of Torr with power deposition of a few W. The microplasma cavity is about 1 mm × 1 mm.

We will discuss scaling laws for the efficiency of VUV photon production in rare gas mixtures of Ar, He, Xe, Kr, and as a function of power format, pressure and cavity sizes.

Work supported by Agilent Technologies.

3-09

Development of a Novel Time-Resolved Laser-Induced Fluorescence Technique

Christopher J. Durot and Alec D. Gallimore

University of Michigan (durot@umich.edu)

We developed a novel technique to interrogate the time-resolved ion velocity distribution function in plasma sources that in steady state operation have some relatively constant spectrum of oscillations, but are not necessarily periodically pulsed, such as Hall thrusters. The system was validated using a hollow cathode as a test bed with an oscillation in discharge current on an anode [1]. Measurements of the new system were validated by comparison with average LIF measurements from a lock-in amplifier and by comparison to an independent time-resolved analysis technique on the same data set.

Of the many oscillations known to affect Hall thrusters, the typically dominant oscillation is known as the breathing mode, which is characterized by an oscillating depletion and replenishment of neutrals at a frequency of about 10-25 kHz [2]. Hall thruster studies have usually focused on time-averaged plasma properties. Such research is reaching maturity while many questions remain about time dependent behavior, such as how the Hall thruster breathing mode and rotating spoke mode affect operation and erosion.

LIF studies using a CW laser often use a lock-in amplifier to recover the fluorescence signal out of the background noise from non-laser-induced emission. The signal-to-noise ratio (SNR) of the raw data is so poor that the lock-in amplifier must be set to an integration time constant of at least 100 ms, destroying time resolution. Examples of recent progress measuring time-resolved LIF in similar plasma sources all employ some form of ensemble averaging triggering off of the phase of oscillation of the plasma discharge current [3], [4].

For the new technique, the laser modulation frequency (~MHz) is above the time scale of interest (10 kHz), allowing band-pass filtering and phase-sensitive detection (PSD) with a short time constant (~μs) to raise SNR and demodulate the signal while preserving time-resolved information. Further averaging is necessary to recover a reasonable SNR due to the short time constant. We have adapted to LIF a technique that was developed for high speed Langmuir probe work involving averaging over transfer functions [5].

The main advantage is the lack of a need for triggering in the time domain. This system can make measurements on thruster operating conditions without a periodic cutoff of discharge current, which was found necessary for triggering in a previous study in a Hall thruster [3]. Another advantage is reduced acquisition time compared to other techniques due to SNR improvement from the combination of fast modulation, filtering, and PSD before averaging.

References

[1] C. J. Durot, A. D. Gallimore, and T.B. Smith, "Development of a Novel Time-Resolved Laser-Induced Fluorescence Technique," Rev. Sci. Instrum., in review.

[2] E. Choueiri, "Plasma oscillations in Hall thrusters," Physics of Plasmas, vol. 8, no. 4, pp. 1411-1426, 2001.

[3] S. Mazouffre and G. Bourgeois, "Spatio-Temporal characteristics of ion velocity in a Hall thruster discharge," Plasma Sources Sci. Technol, vol. 19, no. 065018, p. 9pp, 2010.

[4] N. A. MacDonald, M. A. Cappelli and W. A. Hargus, "Time-synchronized continuous wave laser-induced fluorescence on an oscillatory xenon discharge," Rev. Sci. Instrum., vol. 83, p. 113506, 2012.

[5] R. B. Lobbia and A. D. Gallimore, "Fusing Spatially and Temporally Separated Single-point Turbulent Plasma Flow Measurements into Two-dimensional Time-Resolved Visualizations," in 12th International Conference on Information Fusion, Seattle, Wa, 2009.

3-10

Growth and Analysis of Large Undoped Single Crystal Diamond Substrates using Microwave Plasma-Assisted Chemical Vapor Deposition

Shreya Nad [a], Yajun Gu [a], Jes Asmussen [a.b]

(a) Michigan State University, East Lansing, MI 48824, USA (nadshrey@msu.edu, guyajun@msu.edu)
(b) Fraunhofer USA Inc., Center for Coatings and Laser Applications, East Lansing, MI 48824, USA (asmussen@egr.msu.edu)

Single crystal diamonds (SCDs) play an important role in the semiconductor and electronic industries. Currently commercially available SCDs are limited in size (<1 cm^2) and quality. The long-term objective of this project is to synthesize high quality (<50 ppb N concentration impurity levels, without threaded dislocations and other defects), low birefringence, freestanding (>400 µm) SCD substrates with a grown area of >1cm^2.

Initial experiments have been directed towards the microwave plasma assisted chemical vapor deposition (MPACVD) of high quality single crystal diamond substrates. The growth via MPACVD has been carried out in MSU designed MPACVD reactors B and C. Further description of these reactors are mentioned elsewhere [1], [2]. SCDs have been grown on several 3.5x3.5x1.5 mm^3 Sumitomo HPHT type Ib seeds. Figure 1 shows the top surface of SCD grown in reactor B for 8 hours at a pressure of 240 Torr with 5% CH_4 concentration without any nitrogen addition. The growth rates for these experiments have been within 21–28 µm/hr. Visual analysis of the substrates under optical microscope Nikon 5000D show uniform growth with a step-like deposition. In order to grow large SCD it is necessary to have longer growth times. We have been successful in growing thick (~1.8mm), uniform SCDs in reactor C with 72 hours growth time, 5% CH_4 at a pressure of 240 Torr with a growth rate of ~ 25 µm/hr. Analysis and characterization studies of these substrates using Raman spectroscopy, SIMS, UV-VIS, FTIR and birefringence are in the process.

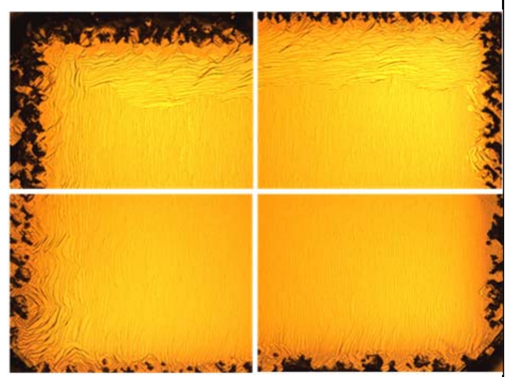

Figure 1 – Uniform step growth of single crystal diamond on 3.5x3.5 mm^2 HPHT seed with a experiment time of 8 hours at 240 T and with 5 % CH_4 concentration.

Future steps involve working with higher pressures (>240Torr), larger HPHT seeds (8X8 mm^2) and simultaneous experiments on multiple seeds. The final step is to design a flip-method which entails flipping the surface by 90º while keeping the growth direction as <100>. This process would enable us to grow large defect-free single crystal diamonds.

References

[1] J. Lu, Y. Gu, T.A. Grotjohn, T. Schuelke, J. Asmussen, Diamond & Relat. Mater. 37 (2013) 17–28
[2] Y. Gu, J. Lu, T. Grotjohn, T. Schuelke, J. Asmussen, Diamond Relat. Mater. 24 (2012) 210.

3-11

The Scaling of Breakdown Voltage of Air Bubbles in Liquid Water

Sarah N. Gucker, Bradley Sommers and John E. Foster

Plasma Science and Technology Lab, Nuclear Engineering and Radiological Sciences,
University of Michigan, Ann Arbor, MI (sngucker@umich.edu)

Radicals produced by the interaction of plasma with liquid water have the capacity to rapidly oxidize organic contaminants, a capability that has garnered world-wide investigation as a method of water purification and sterilization. [1] Direct plasma creation in water typically requires very high voltages to achieve breakdown; however, igniting plasma in individual gas bubbles in liquid water requires much less voltage. [2] The breakdown physics of isolated bubbles in liquid water is still poorly understood. In this work, we investigate the relationship between the applied breakdown voltage and the pressure-electrode distance product, the "pd" of the system. Here, the pd is a range of bubble sizes. This approach allows for the generation of a Paschen-type breakdown curve for isolated bubbles.

References

[1] J. E. Foster, G. Adamovsky, S. N. Gucker and I. M. Blankson, IEEE Trans. Plasma Sci. **41**, 503 (2013).
[2] B. S. Sommers, J. E. Foster, N Yu Babaeva and M. J. Kushner, J. Phys. D: Appl. Phys. **44**, 082001 (2011).

3-12

Creating Magnetized Plasma Jets on the OMEGA Laser

R. P. Young [a], C. C. Kuranz [a], R. P. Drake [a], D. Froula [b], J. Ross [c], C. K. Li [d], and G. Fiksel [b]

(a) University of Michigan (rpyoung@umich.edu, ckuranz@umich.edu, rpdrake@umich.edu)
(b) Laboratory for Laser Energetics (dfroula@lle.rochester.edu, gfik@lle.rochester.edu)
(c) Lawrence Livermore National Laboratory (ross36@llnl.gov)
(d) Massachussetts Institute of Technology (li@psfc.mit.edu)

In April 2012, we had a successful shot day on the OMEGA-60 laser, proving that rear irradiation of thin, conical, acrylic foils can produce a fast, hot, dense plasma jet. We will present a selection of data from that day, focusing on the Thomson scattering data and its implications for fundamental fluid parameters such as Reynolds and magnetic Reynolds numbers. We may also present preliminary data from our recent shot day on August 15, 2013. In that day of experiments, we sought to build upon our success in April 2012 by adding an imposed magnetic field and imaging the magnetized plasma jets with proton radiography.

This work is funded by the NNSA-DS and SC-OFES Joint Program in High-Energy-Density Laboratory Plasmas, grant number DE-FG52-09NA29548, and by the National Laser User Facility Program, grant number DE-NA0000850.

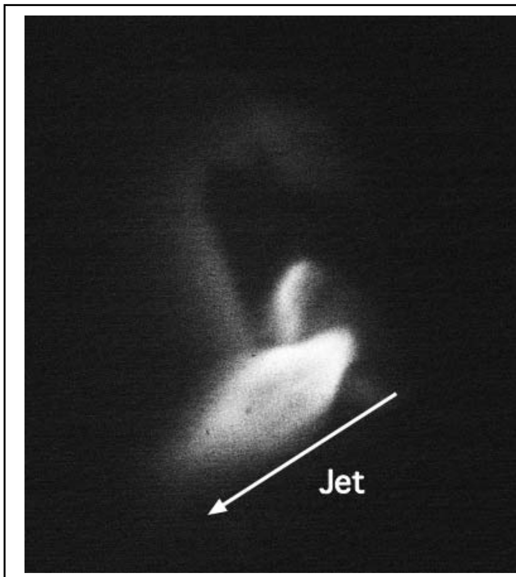

Figure 1 – A jet is clearly evident in this image of self-emission of an experiment from our April 2012 shot day.

3-13

A New Field Solver for Particle-in-Cell (PIC) Methods

Eric Wolf [a], Matthew Bettencourt [b] and Andrew Christlieb [a]

(a) Michigan State University (wolferi1@msu.edu, christli@msu.edu)
(b) Sandia National Labs (mbetten@sandia.gov)

When formulated in terms of scalar and vector potentials in the Lorenz gauge, Maxwell's equations reduce to uncoupled wave equations. A particle-in-cell (PIC) method for the simulation of plasmas may be obtained by coupling these wave equations to the equations of motion of charged particles. We present a new PIC method based on a recently developed fast implicit wave equation solver. This solver is based on the Method of Lines Transpose (MOLT), in which a semidiscrete equation is obtained by discretizing temporal derivatives. An elliptic equation results, which may be solved through a boundary integral method. While a naïve implementation would require $O(N^2)$ operations for N grid points, a fast convolution algorithm was developed for the 1D case that requires only O(N) operations, making it competitive with standard methods for the wave equation. This fast method can be extended to higher dimensions via alternate direction implicit (ADI) splitting.
Using this solver for the wave equations, and explicit leapfrog time stepping for the particles, we develop a PIC method. We consider a quasi-electrostatic case by dropping the vector potential from the model and apply the method to several standard one dimensional electrostatic test problems, finding good agreement with linear theory.

References

[1] C. Birdsall and L. A.B., Plasma physics via computer simulation, Taylor and Francis, New York, 2005.
[2] M. Causley, A. Christlieb, B. Ong, and L. Van Groningen, Method of Lines Transpose: An Implicit Solution to the Wave Equation, Mathematics of Computation, to appear (2013).
[3] M. Causley, Y. Güçlü, E. Wolf, and A. Christlieb, A Fast, Unconditionally stable solver for the wave equation based on the Method of Lines Transpose, Mathematics of Computation, to appear (2013).

An Experimental Study to Show the Effects of Secondary Electron Emission on Plasma Properties in Hall Thrusters

Kapil U. Sawlani and John E. Foster

University of Michigan, Ann Arbor (sawlanik@umich.edu)

The role of secondary electron emission (SEE) in the operation of a crossed field device like a Hall thruster has been a subject of investigation in the recent past. Various physical phenomena are occurring simultaneously when a Hall thruster is operational and the interaction of the plasma with the channel walls of the thruster plays an important role in its effective operation. These secondary electrons derived from electron impact on walls affect plasma transport, which in itself is a complex problem in crossed field devices. The emission of secondary electrons have a nonlinear coupling with the bulk plasma and can affect the wall sheath potential, thereby further impacting the energy transport to the wall.

The emission of secondary electrons from ceramic walls used in channels of Stationary Plasma Thrusters (SPT) have a well-documented influence on its performance and operation. However, this influence is not yet fully understood in the community and thus the computational models are based on assumptions that are not highly accurate. Experimentally, there is no available data on the SEE yield in plasma and its effects to environments similar to that of a Hall thruster, which could be used to validate existing numerical models. Needed is a test-bed apparatus that could serve as a tool to validate and improve existing numerical models by providing the appropriate boundary conditions, secondary yield coefficients and variation of plasma parameters to aid future design of Hall thrusters.

In this work, a bench-top apparatus is used to elucidate the role that secondary electrons play with regards to plasma transport and energy flow towards a Hall thruster channel wall. An electron beam is used to generate a secondary electron plume at the surface of an insulating target. The plasma response to these secondary electrons is assessed by measuring changes to the potential distribution within the sheath of the irradiated target using emissive probes. The changes in the EEDF of the bulk plasma are also measured using Langmuir Probe to understand the influence of these secondary electrons. The sensitivity of these changes to the magnetic field strength is characterized. Also, the variation in the discharge voltage at fixed emission current is determined which yields insight into the crossed field plasma impedance. An attempt is made to relate the findings to the phenomena observed in Hall thrusters.

References

[1] S. Taylor and P. Pix, J. Appl. Phys. **101**, 2389 (2009).
[1] Raitses, Y., Kaganovich, I. D., Khrabrov, A., Sydorenko, D., Fisch, N. J., & Smolyakov, A. Plasma Science, IEEE Transactions on, **39(4)**, 995-1006 (2011),
[2] Sawlani, K. U., Herzog, J. M., Kwak, J. & Foster, J. E., **65th GEC - Texas**, (2012).
[3] G.D Hobbs and J. A. Wesson, Plasma Phys., **9**, 85 (1967).
[4] L. A. Schwager, Phys. Fluids B **5**, 631(1992).
[5] F. Taccogna, S. Longo, and M. Capitelli, Phys. of Plasmas **11**, 1220 (2004).
[6] E. Ahedo, V. de Pablo, M. Martinez-Sanchez, **IEPC-2005-118** (2005).
[7] D. Sydorenko, A. Smolyakov, Y. Raistes, and I. Kaganovich, Phys. Of Plasmas **13**, 014501 (2006).